pH-Indicating Colorimetric Hydrogel for Wound Dressing and Medical Grade Silicone Adhesive for Skin Electronics: Towards Multifunctional Bionic Skin Patch

by

Li Liu

A thesis submitted in partial fulfillment of the requirements for the degree of

Master of Science

in

MATERIALS ENGINEERING

Department of Chemical and Materials Engineering
University of Alberta

© Li Liu, 2016

Abstract

The physiological milieu of the normal skin is slightly acidic with a pH value ranged between 4 and 6; for chronic or infected wounds with a higher bacterial load, its pH value is above 7.3. Motivated by the fact that monitoring the pH value is an effective way to monitor the status of the wound, a novel smart hydrogel wound dressing incorporating modified pH indicator dyes was developed. Phenol red (PR) was used as the dye and successfully modified with methacrylate to allow a copolymerization with the alginate/Polyacrylamide (PAAm) hydrogel matrix. This covalent attachment prevented the dye from leaching out of the matrix. The prepared pH responsive hydrogel dressing exhibited a porous internal structure, excellent mechanical properties and high swelling ratio, as well as appropriate water vapor transmission rate. All these characteristics indicated the hydrogel's suitability for wound dressing materials. The responses of the alginate/P(AAm-MAPR) hydrogel dressing with different calcium and water content were also characterized to consider the case of exudate accumulation into the hydrogel. It was observed that increased calcium content and reduced water content could significantly improve elongation at the break of the hydrogel. The leachability of the dye was evaluated by monitoring the absorbance at 568 nm on a UV-Vis spectrometer. From day 3 to day 7, no loss of the dye was detected, which demonstrated that the covalent attachment of the dye to hydrogel substrate can effectively eliminate the dye leaching problem. The color of the hydrogel dressing underwent a transition from yellow (pH 5, 6 and 7) to bisque (7.4 and 8) and finally to red (pH 9), as pH increased. This range of color change matches the clinically meaningful pH range of chronic or infected wounds. Therefore, the developed hydrogel could be used as a wound dressing to monitor the wound healing process by a simple colorimetric display.

A second aspect of my research involved the exploration of medical grade adhesives,

specifically in combination with surface electromyography (sEMG). Sensors to detect sEMG signals have been widely used by researchers and clinicians in order to capture electrical signals from muscles. While sEMG sensors require an adhesive layer to attach on human skin, the most commonly available ones use acrylic adhesives due to their strong tackiness and low cost. However, the acrylic adhesives are not reusable, difficult to remove and cause skin stripping in some individuals. In addition, they have a tendency to leave residues on skin. Therefore, the adhesion performances of several commercial medical grade silicones were evaluated to find non-irritative alternatives to acrylic adhesives. The silicone adhesives were tacky, non-toxic, non-irritative, and residue-free after removal. Moreover, they were easily washable and allowed multiple cycles of adhesion/debonding. These advantages render the material to be an ideal solution for prolonged use of the electronic patch. Quantitative analyses on the adhesive performances, including peel strength, reusability, and durability, were performed in this research.

Key words: hydrogel wound dressing, pH responsive dye, molecular modification, mechanical test, silicone adhesives, human skin application

Preface

(Mandatory due to collaborative work)

Researches on the skin adhesive, presented in Chapters 4 and 5, were conducted as a part of research collaboration, led by Professor Jana Rieger in Faculty of Rehabilitation Medicine. Experimental methods in sections 4.3.4, 4.3.5, 4.3.6 and 4.3.7 were designed by Kristina Kuffel and Dylan Scott, who provided experimental equipment and supplies. Clear Surgical Tape®, Band-Aid®, and original Acrylic Pad® used in section 4.3.1 are acrylic adhesives; Nexcare Sensitive Skin Tape® and Reusable Self Adhesive® used in section 4.3.1 are silicone adhesives. All the data analysis in chapter 5 were my original work, as well as literature review and experimental evaluation in chapter 4. A summarized form of chapters 4 and 5 will be submitted to a peer-reviewed journal in November.

Researches on hydrogel wound dressing are described in Chapters 2 and 3. The content will be submitted to a peer-reviewed journal in October. Section 6.2.1 in chapter 6 forms a part in a book chapter, "Tough Hydrogels: Toughening Mechanisms and Their Utilization in Stretchable Electronics and in Regenerative Medicines" in the book "Hybrid Material and Interfaces" (Ed. By Marie Helene Delville & Andreas Taubert; Wiley, in press). Dr. Hyun-Joong Chung was the supervisory author of the book chapter, co-authored with three graduate students including myself; Dr. Chung planned, assigned, collected and edited the contents.

Acknowledgements

First and foremost, I would like to thank my supervisor, Dr. Hyun-Joong Chung for providing me with the opportunity to complete my master thesis at the University of Alberta. He has always been available to advice and support. I am very grateful for his patience, inspiration and immerse knowledge in the areas of expertise.

I would like to thank Dr. Jana Rieger for her enthusiasm, inspiration and guidance to this project. I am also indebted to Dr. Ravin Narain for his valuable advices to the thesis. Specially thanks to Dr. Arno de Klerk for the use of rotary evaporator and Dr. Anastasia Elias for the use of tensile and peel testers.

Many thanks to Dr. Thanh-Giang La for reviewing and comments on the thesis, and Xinda Li for his help with ^{1}H NMR experiments and advise during my project. I would also like to express my gratitude to Kristina Kuffel and Dylan Scott for help with experimental design, equipment and supplies.

I would like to acknowledge the sponsors of the NSERC, CIHR and Alberta Cancer Foundation for financial support for the project. Lastly, I would like to express my thanks to my family for their love and care. They have been a constant source of encouragement and support throughout my life.

Table of Contents

Theme 1. Multifunctional Bionic Skin Patch: pH-Indicating Colorimetric Hydrogel for Wound Dressing

Chapter 1. Introduction 1

1.1 Skin surface pH and wound pH 1

1.1.1 Skin surface pH 1

1.1.2 Wound pH 4

1.1.3 Summary 6

1.2 pH-sensors for wound monitoring application 6

1.2.1 Electrochemical wound pH sensors 7

1.2.2 Colorimetric wound pH sensors 10

1.2.3 Summary 13

1.3 Chronic wound dressing 13

1.3.1 Requirements for an ideal dressing 14

1.3.2 Hydrocolloid dressing 16

1.3.3 Hydrofiber dressing 17

1.3.4 Polyurethane foam dressing 17

1.3.5 Gauze dressing 18

1.3.6 Hydrogel dressing 19

1.3.7 Summary 20

1.4 Polyacrylamide (PAAm) /alginate hydrogel 20

1.5 Objectives 23

Chapter 2. Materials and methods 24

2.1 Materials 24

2.2 Experimental methods 24

2.2.1 Synthesis and characterization of methacryloyl modified phenol red (MA-PR) 24

2.2.2 Preparation of P(AAm-MAPR)/alginate hydrogel dressings 25

2.2.3 Characterizations 26

2.2.4 Mechanical test 26

2.2.5 Swelling ratio test 27

2.2.6 Water vapor transmission test 27

2.2.7 Leaching test 28

Chapter 3. Results and Discussion of Hydrogel Wound Dressing **29**

3.1 Synthesis and characterization of MA-PR 29

3.2 Preparation and characterization of P(AAm-MAPR)/alginate hydrogel dressings ... 32

3.3 Physical evaluation of hydrogel dressings as a function of P(AAm-MAPR) crosslinking density 35

3.4 Investigation of mechanical properties under various calcium and water contents ... 39

3.5 Leaching test 42

3.6 Conclusions 43

Theme 2. Multifunctional Bionic Skin Patch: Medical Grade Silicone Adhesive for Skin Electronics

Chapter 4. Medical Grade Silicone Adhesives: A Non-Irritative Solution for Electronic Patches on Skin **45**

4.1 Introduction 45

4.1.1 Adhesion and tack 45

4.1.2 Requirements of skin adhesives 46

4.1.2.1 Toxicological 46

4.1.2.2 Adhesion requirements 48

4.1.3 Mechanisms of adhesion 48

4.1.3.1 Mechanical interlocking theory 48

4.1.3.2 Diffusion theory 50

4.1.3.3 Electronic theory 51

4.1.3.4 Adsorption theory 52

4.1.4 Adhesive types 54

4.1.4.1 Acrylic adhesives 55

4.1.4.2 Rubber-based adhesives 55

4.1.4.3 Polyurethane adhesives 55

4.1.4.4 Soft silicone adhesives 56

4.1.4.5 Cyanoacrylate adhesives 57

4.1.5 Testing of skin adhesive 57

4.1.5.1 Tacking test 57

4.1.5.2 Peel adhesion test 58

4.1.5.3 Dynamic mechanical analysis test 58

4.1.5.4 Creep compliance 59

4.1.6 Summary 60

4.2 Objectives 60

4.3 Fabrication of silicone-based adhesives 61

4.3.1 Materials 61

4.3.2 Fabrication of Silbione 4717, Silbione 4624 and Silpuran pads 62

4.3.3 Peel strength analysis of the fabricated adhesive pads and commercial adhesive pads 62

4.3.4 Aging test of the fabricated adhesive pads 63

4.3.5 Reusability test of the Silbione 4717 adhesive pads 63

4.3.6 Peel strength analysis of different commercial adhesives used for sEMG device 64

4.3.7 Weight loading test of Scapa RX 1383 S adhesives system 64

Chapter 5. Results and discussion of Silicone Skin Adhesives 66

5.1 Fabrication and characterization of silicone adhesive pads 66

5.2 Comparison of Silbione 4717 and various skin adhesive products 67

5.3 Performance evaluation of Silbione 4717 adhesive pads 69

5.4 Medical grade commercially-available silicone adhesives as alternatives to the Silbione 4717 adhesives 73

5.5 Conclusions 75

Chapter 6. Summary and future work 76

6.1 Summary 76

6.2 Future work 77

6.2.1 Sticky hydrogel 77

6.2.2 Temperature-sensing hydrogel 78

References 79

Appendix 88

List of Table

Table 1. Summary of product information for five commercial adhesives 69

List of Figures

Figure 1.1 Fabrication process to create the pH-sensitive bandage. Sensor components including A) UV-insulating layer B) Ag/AgCl layer C) carbon layer and D) insulating layer. E) Images showing the potentiometric sensor on an adhesive bandage. Reproduced with the permission from [3]. 8

Figure 1.2 The pad printing process of electrode. Reproduced with permission from [41]. 9

Figure 1.3 Fabrication of the pH sensing microfibers. (a) A schematic illustration of the pH sensing hydrogel fibers. (b) Schematic of the fiber fabrication process. Reproduced with permission from [6]..... 11

Figure 1.4 Flexible array-type of sensor layer. Color changes of the immobilized dye was observed from yellow to red as the solution became from acidic to alkaline. Reproduced with permission from [45]..... 12

Figure 1.5 One-step method to synthesize PAAm/alginate hydrogel. Reproduced with permission from [72]. Copyright (2013) American Chemical Society..... 22

Figure 3.1 Synthesis and characterization of MA-PR. (a) Reaction scheme for the preparation of MA-PR. (b) Schematic diagram for the synthesis of MA-PR. (c) ^{1}H NMR spectra of PR (blue) and MA-PR (black). (d) FTIR spectra of PR and MA-PR. (e) A photographic image that shows the colorimetric transition of MA-PR in buffer solutions with pH values from 5 to 9 (from left to right). (f) UV-Vis absorption spectra of MA-PR in buffer solutions with pH values from 5 to 9. (g) A schematic drawing that represents the resonance transition in the MA-PR molecule in acidic (left) and basic (right) environment..... 31

Figure 3.2 Preparation and characterization of P(AAm-MAPR)/alginate hydrogel dressings. (a) The chemical structures and the names of the monomers, the dye and the cross-linker used in the synthesis of the alginate/P(AAm-MAPR) hydrogel dressing. (b) Synthetic strategy and colorimetric transitions of the alginate/P(AAm-MAPR) hydrogel dressing. (c) Photographic images that captured the colorimetric transition of the hydrogel dressing in buffer solutions with pH values from 5 to 9 (from left to right). (d) UV-Vis absorption spectra of the hydrogel dressing while immersed in buffer solutions with pH values from 5 to 9. 34

Figure 3.3 Evaluation of the physical properties of the hydrogel dressings as a function of crosslinking density of the P(AAm-MAPR) network. (a) SEM images of hydrogel dressing with the three crosslinking densities from the surface (1-3) and the cross-section views (4-6): 1 and 4 - high crosslinking density (0.15% MBAA concentration); 2 and 5 - medium crosslinking density (0.1 % MBAA concentration); 3 and 6 – low crosslinking density (0.05 % MBAA concentration). (b) Tensile stress – strain curves, (c) Young's modulus and elongation at break, (d) Swelling ratio and (e) Water vapor transmission rate of the hydrogel dressings with the three crosslinking densities. 37

Figure 3.4 Investigation of the mechanical properties as a function of Ca^{2+} concentrations (a, b) and time-dependant swelling/drying conditions (c, d). (a) Tensile stress-strain curves and (b) Young's modulus and elongation at break values with various calcium concentrations. (c) Swelling ratio and (d) Young's modulus and elongation at break values at various time-dependant swelling/drying conditions. All hydrogels have the MBAA concentration of 0.10%. The original state refers to the synthesis condition that hydrogel was vacuum dried in the oven for 2 hrs at 65 ^{o}C after dialysis of 3 days. 41

Figure 3.5 Leaching of the dye over 7 days of dialysis in deionized water. (a) UV-Vis absorbance spectra of the hydrogel from day 0 (without leaching) to day 7 (leached for 7 days). (b) Absorbance at 568 nm as a function of leaching time. 43

Figure 4.1 SEM images of (a) silicone adhesive and (b) acrylic adhesive after removal. Reproduced with permission from [88]. 56

Figure 4.2 Experimental set up for a weight loading test of Scapa RX 1383 S® adhesives. 65

Figure 5.1 (a). Peel strength of three different commercial medical grade silicones at the thickness range between 600~800 μm. (b). Peel strength of Silbione 4717 at three different thickness ranges. 67

Figure 5.2 Peel strength of Silbione 4717 and its comparison against various commercial skin adhesive products. 68

Figure 5.3 The aging test of Silbione 4717 adhesive in ambient environment for 7 days at room temperature, with relative humidity being 20%. 70

Figure 5.4 Reusability test of Silbione 4717 adhesives. (a) Washing test. (b) Wiping test..... 72
Figure 5.5 The peel strength of various commercial medical grade silicone adhesives..... 74

Figure A-1 (a) The set-up of a 90º peel test. (b) The representative graph of a peel test of a Silbione 4717 adhesive pad. (c) Three overlapping peel tests of Silbione 4717 adhesive pads... 89

Chapter 1. Introduction

The pH value within a wound milieu is an important parameter for therapeutic interventions in wound care because it both reflects and influences numerous fundamental physiological and biochemical processes evolved in wound remodeling [1]. A chronic wound is in an alkaline state before healing process; it progresses to a neutral and then an acidic state as healing evolves. Therefore, pH can play a role as an indicator of the status wound healing [2]. Lots of methods to monitor the pH of the wound have been proposed, mostly based on either electrochemical or colorimetric mechanisms [3-5]. Current challenges for these devices include fragility of the electrode, complexity in output analysis and lack of flexibility to conform the topography and the movement of the wound [6]. Colorimetric pH-responsive tough hydrogel wound dressing has a potential to address many of these challenges. By covalently attaching pH indicator dye molecules to polymeric backbones, the modified hydrogel can display the status of wound healing via a simple color observation. Furthermore, hydrogel wound dressing contains lots of water, thus offering various benefits for wound treatment, such as pain control, secretion absorption, oxygen permeability and good mechanical properties [7].

1.1 Skin surface pH and wound pH

1.1.1 Skin surface pH

Wounds are analogous to building sites, where degradation of dead tissue intercalates with the combination of new structures of extracellular matrix and the covering lining of epithelium. Due to this complex regeneration process, wounds are metabolically very active. Many biochemical

reactions happen in the metabolism during the wound healing processes, which require an optimum pH environment. Therefore, pH is an important parameter for therapeutic interventions in wound-care [1].

Under normal conditions the milieu from the surface of skin is acidic, according to the discovery of Hesus et al. in 1892 [8], which was later confirmed by Schade and Marchionini in 1928 [9]. However, up to recent work, the average skin pH value is inconsistently reported for human forearm, cheek and forehead. The lowest range is given with 4.0-5.5 [10], whereas, the most complete skin pH reported in papers goes from as low as 4 up to 6.3 [11].

According to the literature, numerous endogenous and exogenous factors, such as age, anatomy, genetic background, gender, and moisture, have been reported to influence the pH of skin surface [12, 13]. Firstly, age dependence on the skin pH was reported by Visscher et al. [14]. The skin surface pH is neutral for neonates but it decreases to 5.5 after 4 postnatal days. Experimental results of the skin pH on school children are rather scattered. The pH values increase with age in the age group between 18 and 60 [15]. Secondly, comparing skin pH data from different anatomical sites may not be appropriate because skin surface is not uniform and our hygiene habits vary depending on different body areas and on each person [16]. Thirdly, ethnic and genetic backgrounds have also been reported to vary skin pH. For example, people with darker skin typically have lower pH values when compared to people with fairer skin [17]. Fourthly, sex causes variation in skin physiology; A recent study involving 6 male and 6 female volunteers revealed that women have a higher pH (5.6 ± 0.4) than men (4.3 ± 0.4) [17]. Lastly, skin pH also depends on the environmental moisture. Areas with higher moisture, such as axilla and inguinal regions, have higher pH value [18].

In addition, external factors also have considerable impact on the measured skin surface pH. Skin cleansing is one of the most important aspects. After cleansing the skin with alkaline soaps, the pH value was observed to rise for a few hours. The use of synthetic detergent with the same pH as skin or even tap water, also increases the pH values, but the retention time was noticeably shorter. The temporary skin pH changes were caused by the change in the uppermost layers of the stratum corneum [19, 20]. Topical products, such as deodorants, have been reported to influence the skin pH for a few hours [21]. Occlusive dressings also have effects on the skin pH. Hartmann [22] found that the skin surface pH in healthy volunteers was greatly increased after three days of occlusive dressing application, but the value returned to the baseline upon the removal of the dressing within one day. It can be attributed to the increased ion permeability of the stratum corneum resulting from occlusion, which results in the neutralization of the skin surface that is inherently acidic.

The acidic pH milieu is considered as an important aspect of the skin's barrier function against external chemicals. Several pH-dependant enzymes are involved in the formation of the stratum corneum barrier, especially in the construction of lipophilic components and the destruction of desquamation. The enzymes include β -glucocerebrosidase, acid sphingomyelinase, acid lipases, phosphatases and phospholipases. The enzymes exhibit the highest activity at the pH of 5.6, where the synthesis of the most important ceramides is optimized [23]. Some acid hydrolases, the contents of lamellar bodies, are released form the stratum granulosum/stratum compactum interface into the extracellular space by differentiated keratinocytes. These hydrolases as well as the glucosylceramides and phospholipids influenced by the pH are important in the lamellar arrangement of the barrier lipids [24]. The effect of proteolytic enzymes on the epidermal barrier function was investigated by Leyvraz et al. [25]. They found that mice, when membrane-

anchored channel-activating serine protease (CAP 1) is absent in skin, died within 60 h after birth.

Many researches have proved that low pH values in the extracellular space are important in keratinization and barrier regeneration by regulating the enzyme activity. Therefore, the usage of acid buffer substances may be helpful in the maintenance of the homeostasis of the skin [18].

1.1.2 Wound pH

A wound on skin is the consequence of the damaged integrity of multiple skin layers. To start the healing process, many factors, including local wound conditions, systemic mediators, underlying diseases, and kind of injury, need to be taken into consideration. For an acute (i.e., physiological) wound, its healing is a coordinated process containing three major phases: the initial inflammatory phase, the following inflammatory phase and the last remodelling phase. In contrast to physiological wound healing, a chronic wound is defined as a wound that does not follow three stages of physiological healing; the healing process is trapped in a self-sustaining phase of inflammation [26].

The skin's acidic milieu is easily affected by wound that causes a fluidic mixing with body's internal fluid, whose pH value is 7.4. Generally speaking, it is advantageous for wound to have a low surface pH value to prevent bacterial infection. Most relevant human-pathogenic bacteria proliferate at pH values above 6; their growth is inhibited at a lower pH [27, 28]. Stüettgen and Schaefer's study [29] has confirmed that the pH value of the milieu becomes more alkaline compared to healthy case when bacterial colonisation forms. In other report, Greener et al. [30] collected 19 secretion samples from patients with chronic wound; the pH values were ranging between 7.5 and 8.9. A clinical investigation enrolling 50 patients with chronic leg ulcers

showed a range of pH between 7.3 and 8.9, while the average pH value was 7.7 [31]. Another study in leg ulcers displayed a similar pH range, i.e. 7.5-8.9 [32].

In chronic wounds, the balance between tissue degradation and regeneration is disturbed. At such circumstances, the carbolic process becomes dominate. This results in the plethora of proteolytic enzymes in the chronic wound milieu [1]. Some of these enzymes are proteases, which have the ability to cleave proteins. These proteases have their highest activities at a certain range of pH. For example, cathepsin G shows a maximum activity at pH 7.0; elastase at 8.0; plasmin at 8.0, MMP-2 at 8.0, and neutrophil elastase at 8.3 [33]. In addition, bacteria also produce proteases. As a toxin to the wound, ammonia is produced by both enzymes and bacteria. The ammonia prefers an alkaline environment rather than an acidic one [34]. In the chronic wound, four or more different types of bacteria may be harboured at any given time [35].

Moreover, the pH values in the chronic wounds also influence the oxygen delivery to damaged tissue. Leveen et al. [34] . reported that 50% more oxygen will be released by lowering pH by 0.6 units. When the shift was increased to 0.9 pH units, the release of oxygen was increased by five times. Therefore, in chronic wound with elevated pH, the transportation ability of oxygen is dramatically reduced [36].

To accelerate the wound healing process, the wound surface pH needs to be lowered. According to literature, an intensive number of efforts have been made. In earlier days, acetic acid in 1% and 5% solutions has been extensively used to lower wound pH. Unfortunately, the lowered pH only lasts one hour and then returns to the pre-treatment level [34], thus its effect on bacterial burden management is limited. Other problems like product quality and safety issues also raised concerns on its application. Considering all of adverse effects, acetic acid is currently not applied as a licensed sterile agent for wound care [2].

On the other hand, dressings can be successfully used to modify the pH value of the wound. Their permeability to carbon dioxide would contribute to the lowering of the pH values [37]. Gethin and Cowman [38] used the honey dressing to alter surface pH. In their experiment, the time-dependant evolution of the surface pH and the size of 20 chronic non-healing wounds were monitored over two-week period. It was found that the size did not decrease properly when wound pH is high. When the honey dressing is applied, which has a pH of 3.5, the wound surface pH was significantly lowered, resulted in the reduction of the wound size. Romanelli et al. [39] applied Allevyn foam dressings on granulating leg ulcers; here, wound pH decreased to 6.2 from the original 8.2 after 72 hours. Hydrocolloid dressings was also useful in reducing wound pH [40].

1.1.3 Summary

The skin surface is acidic in normal circumstances, which supports natural barrier function and prevents microbial colonisation. A wound tends to increase the pH value of this milieu. Chronic wounds exhibit an elevated pH range of 7.5-8.9. This alkaline environment influences the proteolytic activity and oxygen delivery ability in an adverse way for wound. In recent developments, wound dressings have been shown to be effective in reducing wound pH, resulting in an accelerated wound healing.

1.2 pH-sensors for wound monitoring application

Recently, skin adhesive or mountable pH sensors have been developed to monitor skin conditions. The mechanical properties of these sensors should match those of human skin so that they can form a conformal contact with skin and do not hinder skin's movement. Existing pH

sensors are based on either electrochemical or colorimetric methods. For electrochemical sensors, they measure the concentration of hydrogen ions by processing electrochemical signals. The other approach, colorimetric sensors, use pH sensitive materials and luminescent or pigment dyes to detect skin pH. In the following part, we will give some examples on both methods and also compare their advantages and disadvantages [6].

1.2.1 Electrochemical wound pH sensors

In 1999, Wang et al. [3] developed a new wearable electrochemical sensor for monitoring the pH of wounds. A set of screen-printed silver/silver chloride (Ag/AgCl) electrodes was embedded to a commercial adhesive bandages (see Fig 1.1). It was modified to perform as a potentiometric cell. The reference electrode came from a polyvinyl butyral polymer (PVB). The working electrode was composed of electropolymerized polyaniline, whose electrochemical potential changed with pH. Polyaniline can be obtained from chemical or electrochemical oxidation of aniline ($C_6H_5NH_2$). Oxidation of this leucoemeraldine ((one of the idealized form of polyaniline; $(C_6H_5NH_2)_n$) form resulted in the formation of iminoquinones ($C_6H_5NH_2$) in its polymer structure. When the solution was acidic, polyaniline was in a partially oxidized form – emeraldine ($([C_6H_4NH]_2[C_6H_4N]_2)_n$). A completely oxidized form, polyp-phenylene iminoquinone, was referred to usually as pernigraniline $(C_6H_4N)_n$. The pH value was monitored by measuring the chemical potential that was determined by the ratio between emeraldine salt (ES) to emeraldine base (EB), which was a result of electrochemical equilibrium between the polymer and the environment.

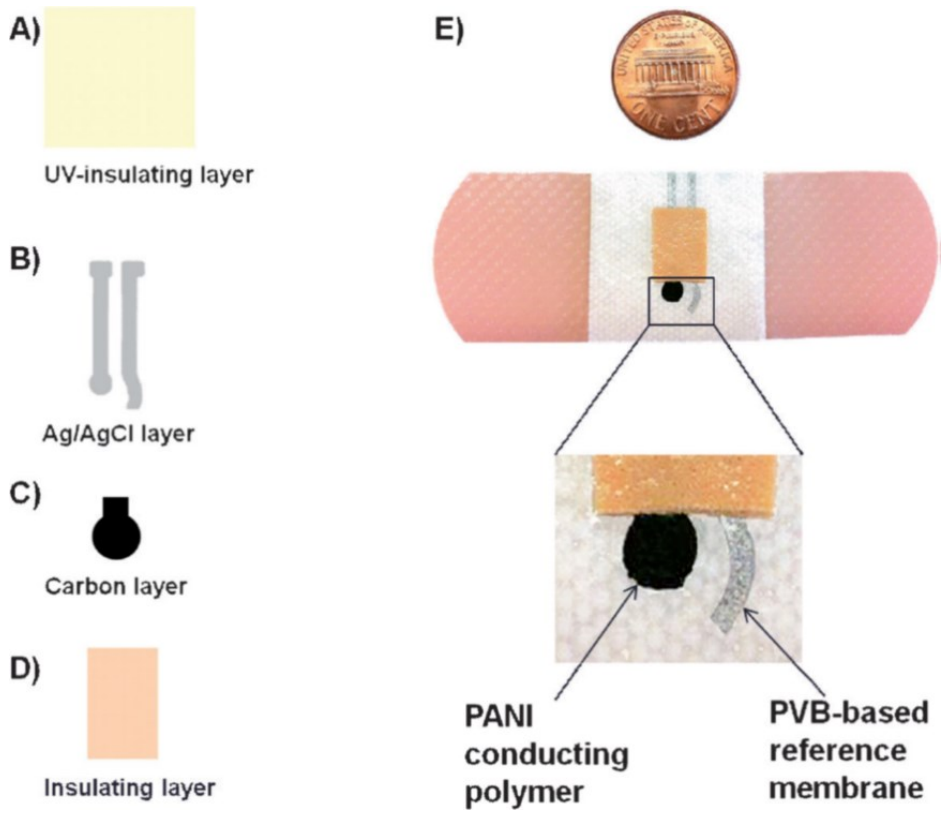

Figure 1.1 Fabrication process to create the pH-sensitive bandage. Sensor components including A) UV-insulating layer B) Ag/AgCl layer C) carbon layer and D) insulating layer. E) Images showing the potentiometric sensor on an adhesive bandage. Reproduced with the permission from [3].

The reported potentiometric sensor combines the screen-printing technology and solid-state potentiometry. It highlights some advantages, such as simplicity, robustness, maintenance-free and low cost. The pH sensitivity is in the range of 4.35-8.0, which well spans the physiological range of interest. The bandage embedded sensor had good resilience against mechanical stress, as well as repeatability, and reproducibility. It is able to track pH fluctuations without apparent carry-over effect. The carry-over effect is that effects from previous treatment may still be present in the new treatment, thus influencing the outcome of the new treatment [3].

Another electrochemical system was developed by Sharp's group [41]. They prepared a pad-printed carbon-uric acid composite sensor to measure pH at the surface of a wound (see Fig 1.2). It was used as biologically-safe pH probe to offer a simple voltammetric response. Electrodes were printed on acetate sheet (transparent film for overhead projector) to provide a flexible printing substrate. The sensor has been proven capable of monitoring pH over a wide analytical range from 4 to 10. Therefore, it might be a powerful tool with clinical utility for wound management. A protective poly-1,2-diaminobenezene coating was deposited on the surface of carbon electrode to prevent biofouling, allowed 20 replicated measurements in a simulated wound fluid.

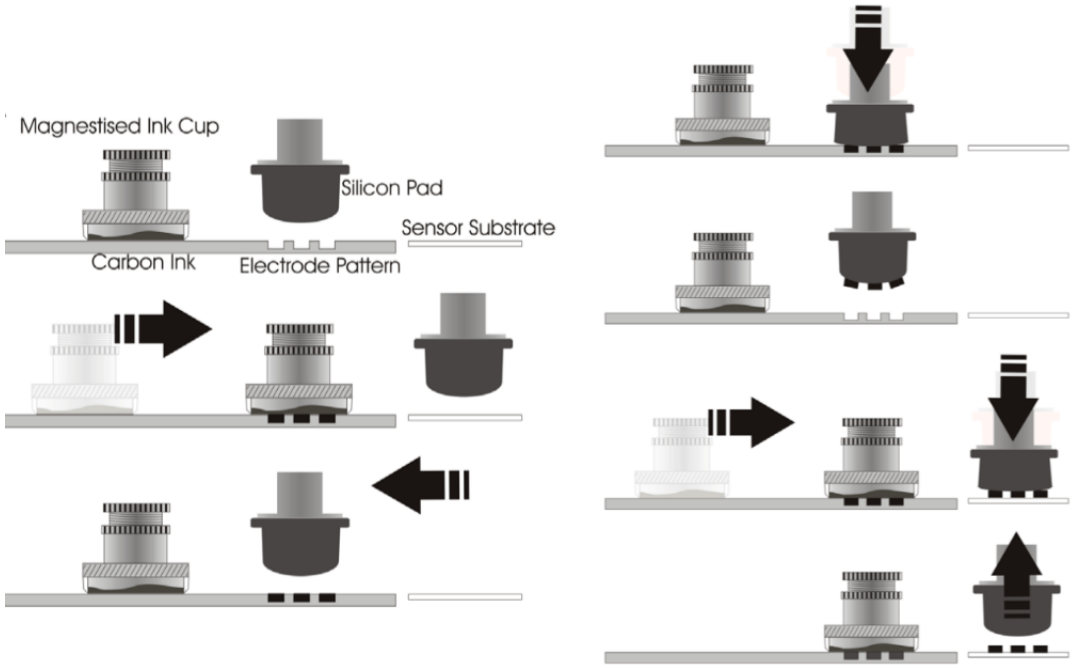

Figure 1.2 The pad printing process of electrode. Reproduced with permission from [41].

The electrochemical technique provides high accuracy and sensitivity towards hydrogen ions in solution as well as reliability and straight forward operation. Various types of electrochemical

sensors have been developed recently, including ion sensors by incorporating selective membranes or metal oxide, ion selective field effect transistors (ISFETs), and conductometric pH sensing devices [42, 43]. However, these sensors suffer from degradation of the sensor performances stemming from mechanical fragility, fouling by non-specific absorption, and requirement of frequent recalibration [4]. In addition, bulky electronic circuitry and power source are required for electrochemical system to analyze the readout [6].

1.2.2 Colorimetric wound pH sensors

Colorimetric sensors display changes in color to represent the concentration or activity of hydrogen ions. Several colorimetric sensors have been proposed for wound pH monitoring. Their working principles are based on either fluorescent chromophore molecules or moieties. Indicator dyes are typically immobilized on the surface of sensor either by covalent linkage or physical entrapment [44]. For example, Khademhosseini et al. [6] reported a flexible pH sensing hydrogel fibres for long-term monitoring of epidermal wound condition. Mesoporous polyester beads were loaded with a pH sensitive dye and subsequently embedded in the alginate-based fibers, which were fabricated in a coaxial flow microfluidic device made from pulled capillaries (see Fig 1.3). The fabricated fibre changed color from yellow to dark red in acidic (pH of 6.2) and basic (pH of 8.2) solutions, respectively.

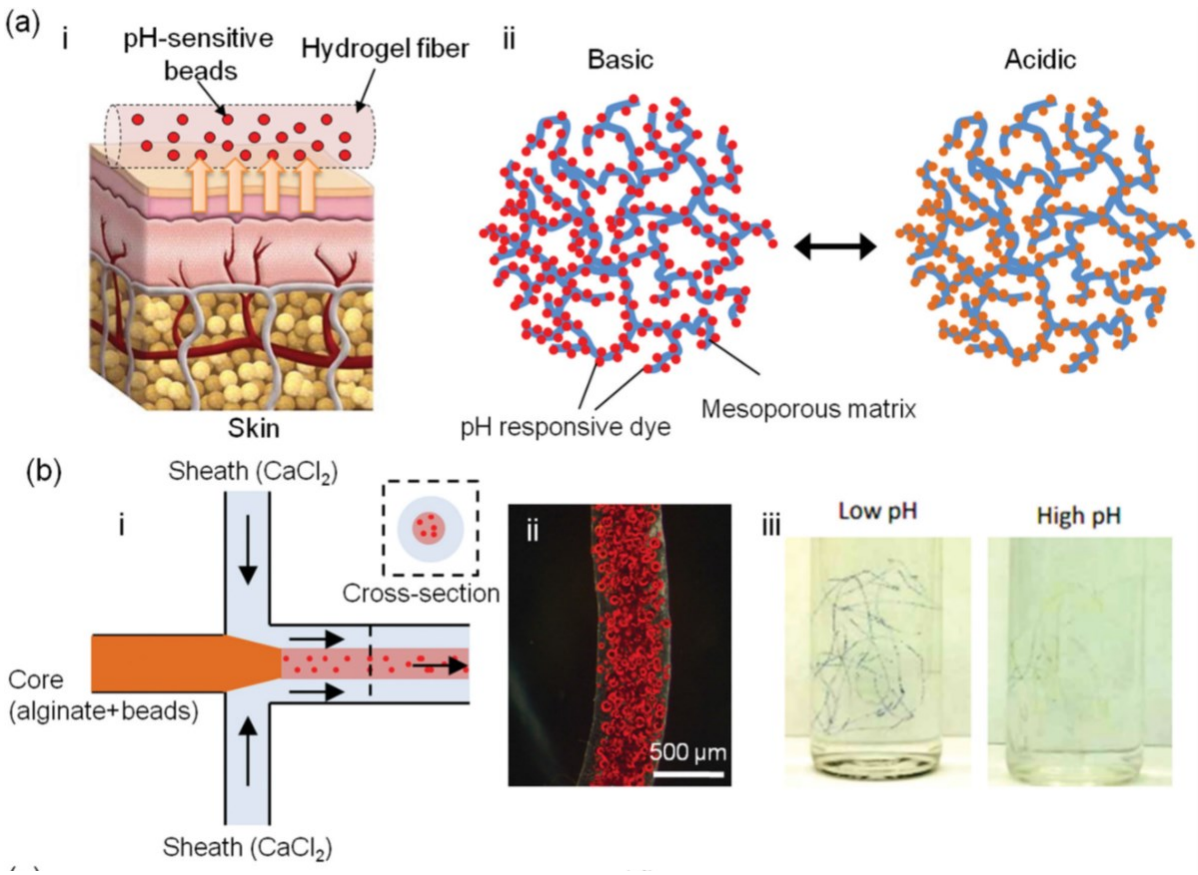

Figure 1.3 Fabrication of the pH sensing microfibers. (a) A schematic illustration of the pH sensing hydrogel fibers. (b) Schematic of the fiber fabrication process. Reproduced with permission from [6].

The fibrous pH sensors are flexible and can be integrated to medical tapes to create a wearable platform. Electrostatic interactions, between the dye and mesoporous particles, efficiently prevent the dye from leaching out of fibers. An image analysis was developed to use a smart phone to determine pH values. These pH sensitive fibers can be easily incorporated to commercial wound dressings to monitor the wound healing process [6].

In other work, Trupp et al. [45] synthesized a series of functional hydroxyazobenzene dyes for optically monitoring pH in the range from 6 to 10 (see Fig 1.4). The sensitivity of the dyes was tailored by substituents in position para or ortho to the hydroxyl group. The indicator dyes were

modified with vinylsulfonyl group and then bond to cellulose films by attacking hydroxyl groups of the cellulose film to achieve covalent bonding. Cellulose film shrivels in aqueous solutions by swelling. Therefore, it is necessary to laminate the film onto a polyethylene terephthalate film, which serves as a passivation layer. The laminated films were patterned into arrays and displayed good reversibility. The array can map the pH distribution across the wounds. As the solution's pH values changed acidic to basic, the film changed its color from yellow to red.

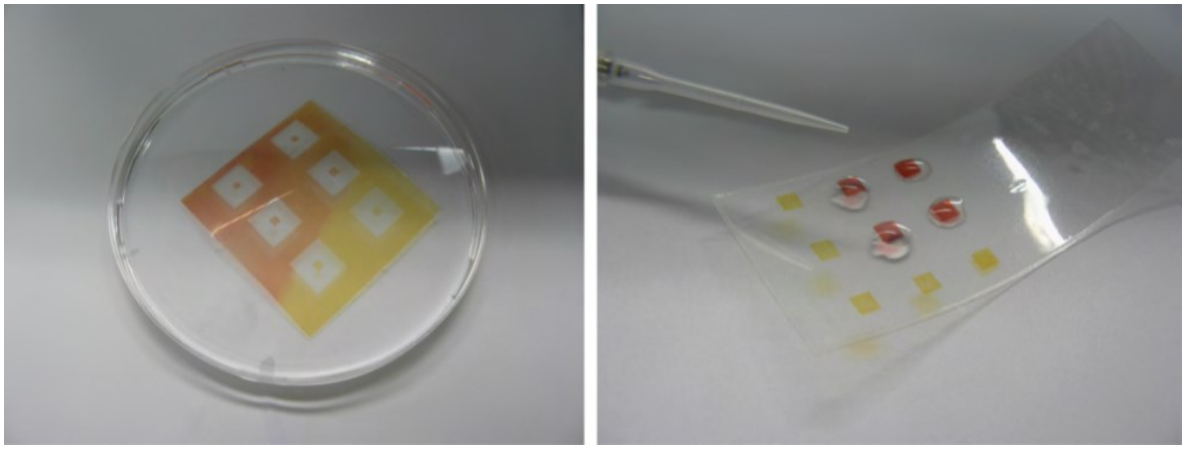

Figure 1.4 Flexible array-type of sensor layer. Color changes of the immobilized dye was observed from yellow to red as the solution became from acidic to alkaline. Reproduced with permission from [45].

Colorimetric monitoring is one of the simplest and most cost-effective methods for wound pH detection [46]. The sensory system is able to display easily visible signal in a non-destructive way without integrated electronics. They can be incorporated into fabric or wound dressings to obtain high flexibility, which is a major advantage over the conventional electronic sensor systems [47]. Currently, the most crucial challenge is that the dyes are easily leached from matrix during operation; the leaching can be toxic to the wound, not to mention that it

compromises the sensitivity. There is plenty room to improve the colorimetric pH sensor for long term practical use in wound monitoring application [6].

1.2.3 Summary

Electrochemical and colorimetric pH sensors have demonstrated their own advantages and drawbacks in wound status monitoring. Electrochemical methods are sensitive and accurate but are fragile, vulnerable to fouling, prone to performance degradation in relatively short time, and requiring frequent recalibration. In comparison, by soling issues related to dye leaching, colorimetric methods can be a more robust and straightforward method to monitor the status of wound.

1.3 Chronic wound dressing

Before 1960, a dry environment was believed to be good for wound healing [48]. Therefore, clinical wound dressing products were intendedly made from cotton or wool for covering and concealing the wound [49, 50]. The importance of dressing materials in the healing process was not fully recognised until the ground-breaking research of by Winter [51]. He found that in a moist environment, epithelialization on porcine wounds occurred two times faster compared to that in a dry environment. This discovery was further confirmed by Hinman and Maibach [52] on human wounds. Since then, people began to realize that dressings are not only functioning as passive coverage, but also actively interact with the wound environment and affect the healing process.

Moist wound environments have many benefits for wound healing. The benefits include enhanced keratinocyte and fibroblast proliferation, keratinocyte migration, collagen synthesis,

angiogenesis, wound contraction, autolytic debridement, and intimate wound closure [53, 54]. However, some clinicians still have concerns about moist wound environments despite the aforementioned strong evidence. In their opinion, wound healing could be improved by a moist environment, however, bacterial growth and subsequent wound infection may also be accelerated by such an environment [55]. To address this concern, Hutchinson and McGuckin [56] performed an experiment in 4000 wounds treated with occlusive (moist) dressings and conventional (dry) dressings. Infection rates showed that conventional dressing exhibited a higher infection rate (7.1%) than occlusive dressings (2.6%). This proved that a moist environment is beneficial to healing as well as a decreased risk of infection.

In the past thirty years, hundreds of dressings have been developed and applied to wounds. Most of them are developed to provide a moist wound environment. In addition to the moist environment, it is important to understand the requirements of an ideal dressing by benchmarking the differences among various dressings so that the criteria for optimum dressing material can be identified for best wound care.

1.3.1 Requirements for an ideal dressing

An ideal wound dressing should be able to guarantee the physical continuity of the wound, absorb excess exudates, protect against infection and external factors, and provide good humidity. In addition, they need to be comfortable when worn and not be allergenic [57].

Water vapor transmission rate (WVTR) is used to measure wound dressings' water retentive ability. It is a measure of the passage of water vapor through a dressing and is qualified by dividing the daily weight loss of water by the area of dressing. A dressing can be regarded as moisture retentive when its WVTR is less than 840 $g/m^2/day$. Different dressings have various

WVTR values, for example, hydrocolloids have a WVTR less than 300 $g/m^2/day$. Gauzes are more prone to water loss, as shown by the WVTR value of 1600 $g/m^2/day$ [54]. A moisture retentive dressing with a low WVTR is especially useful for dry or low-exudating wounds; whereas a more water permeable dressing with a high WVTR is beneficial for wounds with a large amount of exudate. Improper use of wound dressings without considering wound types would result in exudate leakage or wound drying. Frequent dressing change may lead to further physical damage of wounds. As a consequence, clinicians should be familiar with WVTR of different dressings so that the appropriate one can be prescribed for each specific wound [58].

Despite the fact that moist environment is important for wound healing, excessive exudates would result in delayed healing and skin breakdown due to increased wound bacterial loads, as well as periwound skin maceration and wound odor. Therefore, a dressing's swelling capacity should be considered in addition to WVTR [59]. Gentle packing a wound prevents premature wound closure and subsequent abscess formation. However, a wound should not be overpacked because excess pressure can damage fragile tissue [60]. Besides, an ideal dressing should not contain poisonous chemicals and harm the wound bed. Tissue damage should also be avoided upon the removal of dressings. Hence it is necessary for clinicians to find a balance between dressing adherence and atraumatic removal when choosing the right products for wound management [58].

In order to guarantee normal cellular activities, a wound should be kept close to body temperature. This can be achieved by selecting the right retentive dressing and controlling the frequency of dressing changes. Most dressings can stay on the wound up to 7 days, but this varies according to the amount of exudates [59]. And it is also of particular importance for dressings to provide a bacterial barrier to protect against external contamination [58].

Among all the reported works, only a few dressings can satisfy all the requirements to qualify as an ideal one. Therefore, it is necessary to examine wounds type of patient, consider the goal of therapy, review the indications and contraindications for each dressing, and then match the right dressing to wound.

1.3.2 Hydrocolloid dressing

Hydrocolloid dressing is made of carboxymethylcellulose, gelatin, and pectins. It appears in either plate, or hydrocolloid gel form. For plate-shaped dressing, an external layer is required to protect the wound against debris and pathogenic microbial penetration, while the internal layer has hydrophilic carboxymethylcellulose molecules suspending in a hydrophobic mass of gelation and pectin. Meanwhile, hydrocolloid gel form has the same purifying features.

When applied on the wound, hydrocolloids absorb wound exudates and form soft gels. As the gelation process starts, the dressing becomes progressively more permeable to water vapor from the original impermeable state. This permeability lowers the pH and allows the wound to stay at an optimal stable temperature and moisture level. It benefits the successive phases of the wound healing and relieves the pain associated with the existence of wound [61].

Hydrocolloid dressing is indicated for chronic wound with minor or medium amounts of exudates owing to their low WVTR, which is less than 300 $g/m^2/day$. The list of applicable wounds include skin ulcers, burns and abrasions. In addition, hydrocolloid dressing is painless and injury-free during the dressing changing process. Due to the upper water-proof layer, it is possible to wear these dressings even when taking showers. The hydrocolloid dressing is not applicable for infected or necrotic wounds.

1.3.3 Hydrofiber dressing

Hydrofiber dressing is a composite material that mainly contains carboxymethylcellulose. It forms a gel coating on the wound bed by absorbing the exudates into the fibers. Then, the exudates are confined inside of the dressing. The dressing has a high swelling ratio of exudates which is up to 25 times of its original weight. It keeps micro-organisms in the exudates inside the gel so that they can be isolated from the wound. The dressing can also lower the wound's pH value to inhibit bacterial growth and prevent skin irritation around the wound. In addition, it maintains a moist environment for wound and activates angiogenesis and fibrinolysis.

Hydrofiber dressings are good for bacteria-infected wound, and neglected wound with heavy or medium amount of exudates. But they should not be used for dry wound that does not produce significant amount of exudates [62, 63]. A secondary top dressing has to be covered on hydrofiber dressing. When changing dressings, it is painless and injury-free [61].

1.3.4 Polyurethane foam dressing

Polyurethane foam dressing is hydrophilic foam with porous structure containing two layers. One layer is thermally processed to form capillaries to absorb water and to keep the wound at a good moisture level. The other layer is a membrane, which allows water vapor to evaporate from the wound surface while blocking pathogens and water to enter from outside [61]. The WVTR of foam dressings varies widely from 800 $g/m^2/day$ to 5000 $g/m^2/day$ depending on the thickness and composition of the foam [53, 64].

Foam dressing can be applied to wounds with medium or high-level exudates and to granulating or necrotic wounds; it also can be applied to wounds of any etiology. But it is not beneficial on

dry wounds. Friction is decreased by applying foam dressing but its thickness is not enough to reduce pressure in bony prominence area. Besides, it is able to provide protection for autolytic debridement and decrease exuberant granulation tissue.

Adhesive foam dressing should be used carefully for patients with fragile skin. Non-adhesive dressing requires an additional tape or other method to keep the dressing in contact with the wound. These foam dressings should cover minimum one inch of the margin around the wound and get changed at least every 7 days. Thick foams can be wrapped compressively and then used on venous ulcers to increase local compression, aiding in local edema control and healing improvement [58].

1.3.5 Gauze dressing

Gauze is still the most commonly used dressing in wound management nowadays. It consists of natural or synthetic materials, or a mixture of both, and can be woven or nonwoven [65, 66]. Woven gauze is usually for packing. Suitable fibers are made into threads and then weaved into the fabric to produce woven gauzes. Compared to nonwoven gauzes, their swelling ratio is lower and thus easier to dry the wound surface and adhere to wound bed. Nonwoven gauze is made only by blending fibers without thread development. This gauze has a high swelling ratio, thus less prone to adhere to the wound.

Gauze dressing is indicated for wounds with heavy exudates and also used as a primary dressing over ointments, enzymes and growth factors. Besides, it can be applied over wound fillers and hydrogels as a secondary dressing. If the gauze dressing adheres to viable tissue or damage skin upon removal, gauze dressing should not be used any more [58].

There are disadvantages of the gauze dressing. It is helpful in the debridement of necrotic tissue but the debridement is not selective. So the dressing is harmful to the viable tissue when it adheres to the wound. Gauzes have the propensity to dry out the wound; they need to be moistened several times daily to maintain a wet environment for wound, which is time- and labour-consuming. Furthermore, cotton fibers left in the wound site may lead to inflammation and slow wound healing [67].

1.3.6 Hydrogel dressing

Hydrogel has a three dimensional network structure that can contain lots of water. Amorphous gel packed in tubes, foil packets, or as saturated gauze pads is available for sterilization and for single or multiple uses when preserved. Alginate, collagen, and starch copolymer are incorporated into hydrogel to provide some exudate absorption. These dressings are mainly for wound hydration.

Hydrogel dressing can be used to clear the ulcer of necrotic tissue and micro-organisms by binding them into the gel structure. The moist environment provided by the hydrogel stimulates the growth of new tissues and the migration of epithelial cells. Pain can be decreased by cooling the wound site. In addition, the hydrophilic features of the hydrogel can moisten dry wound bed, dissolve crust/black necrosis and activate lyses in the wound. Therefore, hydrogel wound dressing can be applied to dry or minimally-exudating wounds. Amorphous gel may be applied on infected wounds; in this case, the dressing must be changed everyday. But hydrogel dressing should not be applied to wounds with heavy exudate.

Hydrogel is typically non-adhesive and easy to conform on wound bed. However, the dressing may cause maceration for periwound skin. Some of the hydrogel dressings lack sufficient levels

of humectants, thus may dry out when applied to the wound. The frequency of the dressing change is related to the moisture level of the wound. If the wound dries out in one day, the dressing has to be changed daily. But if they are able to keep the wound hydrated for a longer time, the changing frequency can be lessened. Sometimes a secondary dressing is necessary for the amorphous hydrogel to keep wounds at an appropriate moist level. Gauze may be used as secondary dressing for wounds with some exudates and inherent moisture, while less permeable dressings is preferred for wounds that tend to dry out [58].

1.3.7 Summary

Hundreds of dressings have been developed over the past several decades; thus it is important for clinicians to know the requirements of an ideal dressing according to the class of wounds. These requirements include the maintenance of a moist wound environment, absorption of excess exudates, elimination of the dead tissue, and provision of bacterial barrier. The goal of care for an individual patient and wound should also be identified, so that the most appropriate dressing can be selected from many dressing categories to accelerate wound healing.

1.4 Polyacrylamide (PAAm) /alginate hydrogel

Hydrogel has been explored in a variety of biological applications, such as regenerative medicine, drug delivery, stem cell and cancer research as well as cell therapy. Hydrogel has tunable physical, chemical and biological properties, high biocompatibility, ease of fabrication, and similarity to native extracellular matrix. However, the application of the hydrogel in medicine has always been limited to applications that do not require physical integrity due to its

weak mechanical strength [68-70]. Mechanically strong hydrogel has the potential to expand the applications towards those that require significant load-bearing and agile movements.

Suo's group [71] at Harvard University developed an extremely stretchable and tough hydrogel by creating an interpenetrating networks of PAAm/alginate hydrogels. These hydrogels are crosslinked by covalent and ionic molecular forces, respectively. The ionically crosslinked alginate chain contains mannuronic acid (M unit) and gulutonic acid (G unit), arranged in blocks rich in G units, blocks rich in M units, and blocks of alternating G and M units. Calcium ions are used to crosslink the G blocks in different chains to form alginate hydrogel in aqueous solution. In contrast, the polyacrylamide hydrogel was crosslinked by agent that promotes network formation by covalent bonding.

The PAAm/alginate hydrogel was fabricated by a one step method through mixing all of the ingredients dissolved in water. Sodium alginate and calcium chloride were used to form ionically crosslinked alginate; acrylamide, covalent cross-linker (N,N'-methylenebisacrylamide, MBAA), thermo-initiator (ammonium persulphate, APS) and accelerator (N,N,N',N'-tetramethylethylenediamine, TEMED) were used to form PAAm network. As a consequence, alginate chains interpenetrate into the network of covalently crosslinked PAAm chains, while the two hydrogels are formed concurrently [72]. The schematic diagram is illustrated in Fig 1.5.

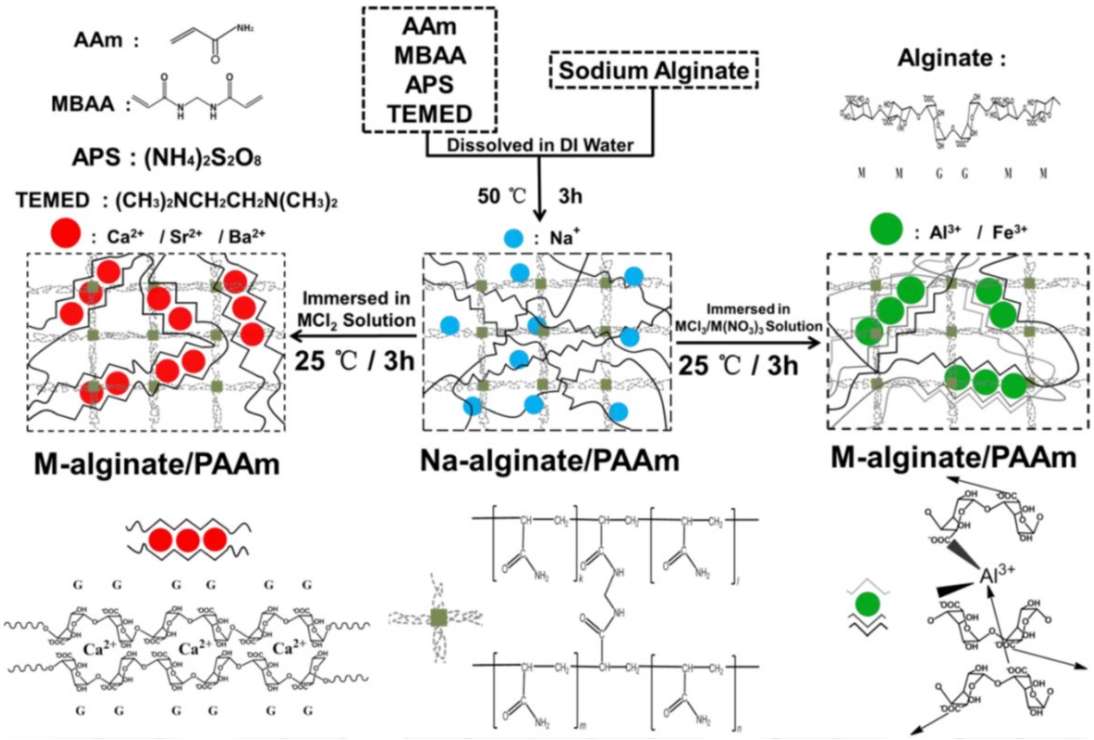

Figure 1.5 One-step method to synthesize PAAm/alginate hydrogel. Reproduced with permission from [72]. Copyright (2013) American Chemical Society.

Even though this hydrogel has a high content of water (~ 90%), it can withstand a great amount of strain up to 20 times its initial strength. The hydrogel's fracture toughness can be up to 9000 J m^{-2}. This value is dramatically higher compared with that of the pure alginate hydrogel (~25 J m^{-2}) and pure PAAm hydrogel (~150 J m^{-2}) [71]. The remarkable toughness of hydrogel can be explained as follows. When the hydrogel is subjected to a small stretch, the elastic modulus of the hydrogel is the sum of those of alginate and PAAm hydrogels. The applied load is distributed to both of the hydrogels because the two polymers are entangled. Possible crosslinks between the amine groups on PAAm chains and carboxyl groups on alginate chains further facilitates the load sharing. As the stretch progresses, the loosely crosslinked PAAm (i.e., long chain length between crosslinking points) chain remains intact and stabilizes the hydrogel under deformation, while

the alginate network is unzipped in a reversible manner by the break of ionic bonding between the polymer chains, which offers an efficient mechanism for energy dissipation [71].

The high water content, high toughness, good stretchability, and structural resilience, along with easy method of synthesis, render PAAm/alginate hydrogel an ideal candidate for applications, such as artificial tissues, soft robotics, and structural materials [73]. In my thesis, I focused on the possibility of applying the hydrogel to wound dressing.

1.5 Objectives

The objective of theme 1 is to develop a pH indicating colorimetric tough hydrogel alginate/PAAm for a smart wound dressing application. The pH indicator dye phenol red was modified with methacryloyl moiety to allow the modified monomer to participate in the radical polymerization reaction of PAAm so that it can be covalently incorporated in the hydrogel network. Since unmodified dye will not be anchored to the hydrogel matrix, subsequent dialysis can naturally remove the unattached dye, which can potentially be cytotoxic. Furthermore, covalent attachments of the dye can possibly eliminate the problems associated with leaching under prolonged use of the hydrogel as wound dressing. The prepared alginate/P(MAPR-AAM) hydrogel dressing was flexible, moist, mechanically strong and can indicate the progress of wound healing by a simple colorimetric display.

Chapter 2. Materials and methods

2.1 Materials

Phenol red dye, methacryloyl chloride, triethylamine (TEA), anhydrous tetrahydrofuran (THF), dimethyl sulfoxide (DMSO), ammonium persulphate (APS), N, N'-methylenebisacrylamide (MBAA), acrylamide (AAm), N, N, N', N'-tetramethylethylenediamine (TEMED), calcium chloride ($CaCl_2$) and sodium alginate were purchased from Sigma-Aldrich and used as received. Potassium sodium buffer solutions with pH values of 5, 6, 7, 7.4, 8 and 9 were obtained from Fisher Scientific. All other chemicals used in this work were used as received.

2.2 Experimental methods

2.2.1 Synthesis and characterization of methacryloyl modified phenol red (MA-PR)

A mixture of phenol red (0.5 g, 0.0014 mol) and triethylamine (250 µL, 0.0018 mol) was dissolved in 40 mL anhydrous tetrahydrofuran, and the mixture was kept in an ice bath. Afterwards, a solution of methacryloyl chloride (136.8 µL, 0.0014 mol) in 10 mL anhydrous tetrahydrofuran was added dropwise to the above mixture slowly under N_2 atmosphere. After the addition of methacryloyl chloride, the resultant mixture was stirred overnight. The solid was filtered and the solvent was removed by rotary evaporation. The red modified dye powders were obtained.

The chemical structure of MA-PR was confirmed by Fourier transform infrared spectroscopy (Nicolet 8700, Nicolet Instrument Co., WI). To obtain FTIR spectra, the dye powders were

mixed with dry KBr powders and then loaded into the sample holder. The resolution was 2 cm^{-1} and the sample was scanned from 4000 to 400 cm^{-1} for 64 times. The ^{1}H NMR spectra was recorded on a VNMRS 600 MHz spectrometer with DMSO-d_6 being the solvent. Chemical shifts were recorded in ppm and referenced against tetramethylsilane (TMS). MA-PR powders were dissolved in buffer solutions from pH 5 to pH 9 to observe the color changes. Mechanism was explained by UV-Vis spectroscopy. The cuvette with MA-PR buffer solution was placed in the sample compartment of the UV-Vis spectrophotometer (Perkin-Elmer NIR-UV, PerkinElmer, USA) and the UV-Vis spectrum was recorded.

2.2.2 Preparation of P(AAm-MAPR)/alginate hydrogel dressings

The hybrid hydrogel was synthesised by two steps following to the method developed by Zhou et al. [73]. Firstly, Sodium alginate (0.1 g), modified dye MA-PR (0.001 g) and acrylamide grain (0.8 g) were dissolved in 5 mL deionized water. MBAA (0.0008 g, 0.1 wt % to AAm), as the crosslinking agent, and APS (0.0008 g, 0.1 wt% to AAm), as the thermos-initiator, were subsequently added into the solution. The mixture was stirred to become homogeneous solution and then degassed under vacuum for 20 mins to remove air bubbles. After adding the accelerator TEMED (5 µL), the solution was transferred into a glass mould and then incubated in an oven at 70 ^{o}C for 3 hours. This step produced a Na-alginate/P(AAm-MAPR) hydrogel. Secondly, the Na-alginate/P(AAm-MAPR) hydrogel was soaked in 2 wt% $CaCl_2$ solution (0.2 g $CaCl_2$ in 10 mL H_2O) for 3 hours at room temperature to crosslink the alginate. Afterwards, the synthesized P(AAm-MAPR)/alginate hydrogel dressing was dialysed for 3 days to wash away unreacted monomers and dried in a vacuum oven at 65 ^{o}C over 2 hours. The blank hydrogel without MA-PR dye was also synthesized as the control group using the same recipe.

A series of P(AAm-MAPR)/alginate hydrogels with 0.05 wt% MBAA (0.0004 g), 0.1 wt% (0.008 g), 0.15 wt% (0.0012g) were prepared. Amounts of other chemicals were kept the same as used in the above recipe. Similarly, hydrogels with 0.1 wt%, 1 wt%, 2 wt%, 5 wt% $CaCl_2$ were synthesized by only adjusting the amount of $CaCl_2$ to be 0.01 g, 0.1 g, 0.2 g, 0.5 g in 10 mL H_2O, respectively.

2.2.3 Characterizations

The morphologies of the as-synthesized P(AAm-MAPR)/alginate hydrogels with different concentrations of MBAA were observed with a scanning electron microscope (SEM) (Zeiss EVO MA10, Zeiss, Germany). After the hydrogel was immersed in deionized water for 1 day, it was rapidly frozen in liquid nitrogen at -40 ^{o}C and lyophilized at -50 ^{o}C for 24 h in a SuperModulyo freeze dryer (Thermo Savant, NY, USA). The swollen freeze-dried sample then was mounted onto an aluminum stub and sputter-coated with gold for SEM observation. P(AAm-MAPR)/alginate hydrogels were soaked in buffer solutions with a pH value from 5 to 9 to observe the color changes. Mechanism was explained by UV-Vis spectroscopy. The buffer solution-soaked hydrogels were cut into strips to fit in the cuvette and subsequently placed in the sample compartment of the UV-Vis spectrophotometer (Perkin-Elmer NIR-UV, PerkinElmer, USA) and the UV-Vis spectra were recorded.

2.2.4 Mechanical test

The mechanical properties of the prepared hydrogel dressings with various water contents and crosslinking densities were measured using an Instron 5943 tensile tester equipped with 10 kN

load cell at room temperature. The hydrogels were cut into strips with dimension of 6 cm × 1 cm × 0.1 cm. Both ends of the sample were gripped with a special gripper with a crosshead speed of 100 mm · min. Young's modulus (E) was measured from the slope of the linear section of the stress-strain curve. The elongation at break was calculated by comparing the length of the hydrogel at the breakage to the initial length of the hydrogel. Six measurements were repeated for each sample to obtain the average value.

2.2.5 Swelling ratio test

The hydrogel dressing samples with three different MBAA concentrations (0.05 wt%, 0.1 wt%, 0.15 wt%) were cut into 2 cm × 2 cm squares and dried at 65 ^{o}C under vacuum for 24h. Subsequently, they were immersed in phosphate buffer solution (PBS, pH 7.4) at 37 ^{o}C for 72 h until equilibrium. At specific time intervals, the excessive surface water was removed with filter paper, and the weights of samples were measured. All the measurements were conducted three times to confirm the values. The swelling ratio (SR) was determined using the equation SR%= $(W_s - W_d)/W_d \times 100$; where W_s and W_d are the weights of the hydrogel sample swollen in PBS at 37 ^{o}C and dried for 24 h at 65 ^{o}C, respectively.

2.2.6 Water vapor transmission test

The water vapor transmission rates (WVTR) of hydrogel dressings with three different MBAA concentrations (0.05 wt%, 0.1 wt%, 0.15 wt%) were determined according to the ASTM E96 standard method. Briefly, the hydrogel dressings were mounted and sealed on the top of opened vials (diameter of 17 mm) containing 20 mL deionized water. Barrier tapes were used to tightly

fasten the hydrogel dressings. The hydrogel-vial assemblies were placed in an isothermal incubator at 37 ^{o}C for 72h. Periodic weightings were carried out to measure the water evaporation through the hydrogel dressings. The measurement was repeated three times for each sample. The WVTR was determined by dividing the daily weight loss of water with the area of vial opening.

2.2.7 Leaching test

The degree of dye leaching was determined by monitoring the absorbance at 568 nm on a UV-VIS spectrometer (Perkin-Elmer NIR-UV, PerkinElmer, USA). The hydrogel dressings were prepared to be strip samples with dimension of 1cm × 3 cm and stored in deionized water for 7 days. The water for dialysis was changed everyday. The blank PAAm/alginate (dye-free) gel was measured as a control sample; its spectrum was used for background subtraction. Absorbance spectra of P(AAm-MAPR)/alginate hydrogel samples were also obtained from day 0 (without leaching) to day 7 (leached for 7 days). All measurements were performed three times. The value of absorbance of P(AAm-MAPR)/alginate hydrogel at 564 nm was plotted against the time of leaching.

Chapter 3. Results and Discussion of Hydrogel Wound Dressing

3.1 Synthesis and characterization of MA-PR

The pH indicator dye, phenol red (PR), consists of three benzene rings with one sulfonate group and two hydroxyl groups that render pH-sensitivity. Nucleophilic substitution of one hydroxyl group on PR dye with methacryloyl chloride results in the formation of a methacryloyl functional dye, MA-PR. The reaction scheme and the concept of the functionalization are depicted in Fig. 3.1 (a) and (b), respectively. The one step modification was simple and straightforward to perform. After the reaction, the crude product was isolated from THF solvent by rotary evaporation. Further purification was not necessary because MA-PR will be covalently anchored to the hydrogel matrix in the following copolymerization, while the residue PR was free to diffuse out of the matrix by dialysis [74].

FTIR and ^{1}H NMR spectroscopies were used to reveal the chemical structure of synthesized MA-PR. ^{1}H NMR spectroscopy is illustrated in Fig 3.1 (c); here the spectrum of PR was compared with that of the MA-PR. The peak at 1.81 ppm (7) was assigned to the protons of CH_3 of methacryloyl group. The two singlets at 5.57 (9) and 5.94 ppm (8) were assigned to the vinyl protons of CH_3-C=CH_2*; the splitting could be attributed to the conjugation of carbonyl and vinyl group. This conjugation limited the mobility of double bonding and, consequently, the two protons on the vinyl group experienced different chemical environments to each other. The multiple peaks in the range of 6.74 – 8.02 ppm were assigned to the protons in the aromatic rings. The results of ^{1}H NMR indicated that unsaturated C=C bonds were successfully introduced to PR in the MA-PR.

FTIR spectra from PR and MA-PR FTIR were compared in Fig 3.1 (d). They both exhibited a phenol band of PR and MA-PR consisting of two components: a broad band centered at 2967 cm^{-1}, attributed to hydrogen-bonded phenol groups, and a relative narrow band at 3584 cm^{-1}, assigned to free phenol groups. The typical stretching absorption of carbonyl group in the methyl methacrylate structure was located at 1739 cm^{-1}; only MA-PR spectrum exhibited the peak. The peak at 1671 cm^{-1} was originated from the C=C stretching of the vinyl structure and multiple peaks from 1460 – 1640 cm^{-1} were due to the C=C stretching of aromatic rings. Bands at 1156 and 1366 cm^{-1} were resulted from stretching vibrations of sulfonate groups. In summary, the results of ^{1}H NMR and FTIR confirmed the modification of MA-PR dye was as I designed.

MA-PR dyes displayed a distinct color variation in buffer solutions with five different pH values. With increasing pH, the MA-PR dyes underwent a transition from yellow (pH 5) to orange (pH 7) and finally to magenta (pH 9), as shown in Fig 3.1 (e). The color changes were quantitatively displayed in the UV-vis spectra as a function of pH, as shown in Fig 3.1 (f). Here, the MA-PR showed maximum absorbance peaks at 388 nm in acidic conditions. The peak intensity decreased as pH became more basic, and a peak at 588 nm emerged. The 588 nm peak corresponded to the deprotonated form of the dyes, which became abundant as pH increased. The transition in the dominant peak was due to the resonance transformation in the molecular structure of MA-PR, as schematically described in Fig 3.1 (g). The peak at 388 nm was attributed to the π-π^* transition of the conjugated benzenoid ring system. When the solution became more alkaline, the new absorption band at 558 nm was assigned to the n-π^* transition resulting from benzenoid to quiniod excitonic transformation.

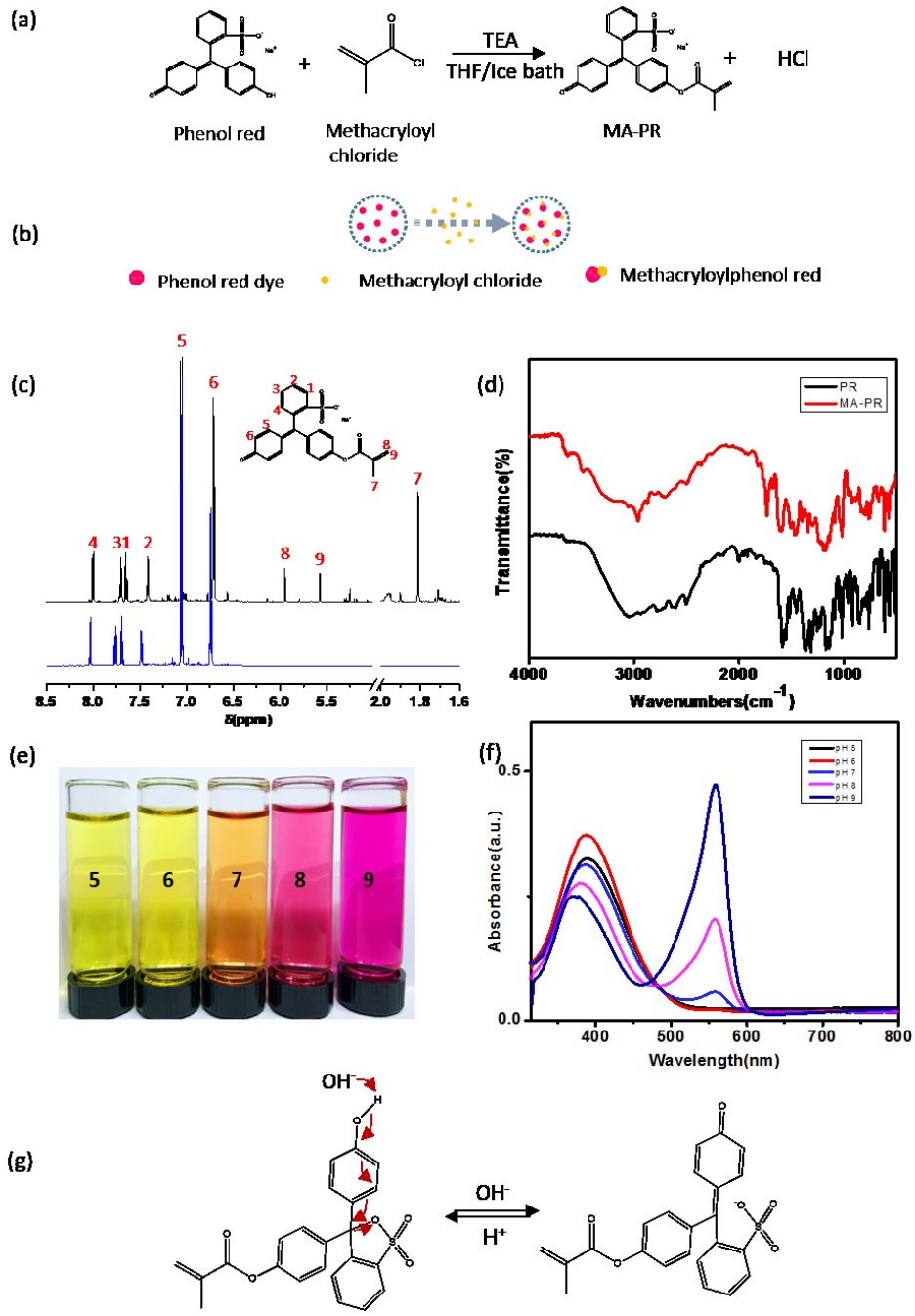

Figure 3.1 Synthesis and characterization of MA-PR. (a) Reaction scheme for the preparation of MA-PR. (b) Schematic diagram for the synthesis of MA-PR. (c) ^{1}H NMR spectra of PR (blue) and MA-PR (black). (d) FTIR spectra of PR and MA-PR. (e) A photographic image that shows the colorimetric transition of MA-PR in buffer solutions with pH values from 5 to 9 (from left to right). (f) UV-Vis absorption spectra of MA-PR in buffer solutions with pH values from 5 to 9. (g) A schematic drawing that represents the resonance transition in the MA-PR molecule in acidic (left) and basic (right) environment.

3.2 Preparation and characterization of P(AAm-MAPR)/alginate hydrogel dressings

The P(AAm-MAPR)/alginate hydrogel dressing was synthesized by a two-step approach including the synthesis of MA-PR dye and the synthesis of the double network hydrogel. To fabricate the hydrogel dressing, all ingredients were mixed in water to form the two interpenetrating hydrogel networks: sodium alginate and crosslinker $CaCl_2$ for the ionically crosslinked alginate; monomer AAm and MA-PR, crosslinker MBAA, thermoinitiator TEMED for the covalently crosslinked P(AAm-MAPR). The chemical structures and names of the monomers, the dye and the crosslinker are presented in Fig 3.2 (a). As a result, the loosely crosslinked long PAAm polymer chains interpenetrated with the densely crosslinked Ca-alginate to develop a tough double network hydrogel [73]. Schematic diagram is illustrated in Fig 3.2 (b). The high mechanical strength of this hydrogel could be described as following [71]: when the load was applied, the loose PAAm network remained intact and stabilized the deformation; meanwhile, alginate networks unzipped progressively. The closely spaced ionic crosslinks unzipped at small stretch, but the ionic bonding was reversible and non-specific. Therefore, the unzipping of ionic bonding dissipated fracture energy in an efficient way.

A transparent medical tape was adhered on one side of the pH-responsive hydrogel dressing to create a wearable platform on wound. Subsequently, the dressing was soaked in buffer solutions with various pH values (pH = 5, 6, 7, 7.4, 8, 9). The color of the hydrogel dressing underwent a transition from yellow (pH 5, 6 and 7) to bisque (7.4 and 8) and finally to red (pH 9), as captured by a smartphone photography in Fig 3.2 (c). The pH window of the color transition matches the pH range that is required to display the status of chronic or infected wounds. As the wound heals, its chronic environment progresses from an alkaline condition to a neutral and then an acidic

condition [2], and the hydrogel dressing turns from red to bisque and then to yellow. Fig 3.2 (d) illustrates the UV-Vis absorbance spectra of the MA-PR in the hydrogel dressing after exposed to different pH buffer solutions. In acidic buffer, only one absorption peak was observed at 427 nm, similar to the case of the free MA-PR dye in solutions. When the pH varied from acidic to basic, the absorption started to undergo a red shift, as qualified by the decreasing intensity of the 427 nm peak and by the increasing intensity of 573 nm peak, which was the result of the resonance transition. A quantitative comparison of the MA-PR peaks between the free and the hydrogel states showed that the most hypsochromic maximum wavelength shifted from 388 nm (free) to 427 nm (hydrogel), whereas the most bathochromic wavelength shifted from 558 nm (free) to 573 nm (hydrogel). A possible explanation was that the interactions between the dye and the hydrogel lowered the excitation energy of MA-PR molecules when they were covalently immobilized within the hydrogel networks.

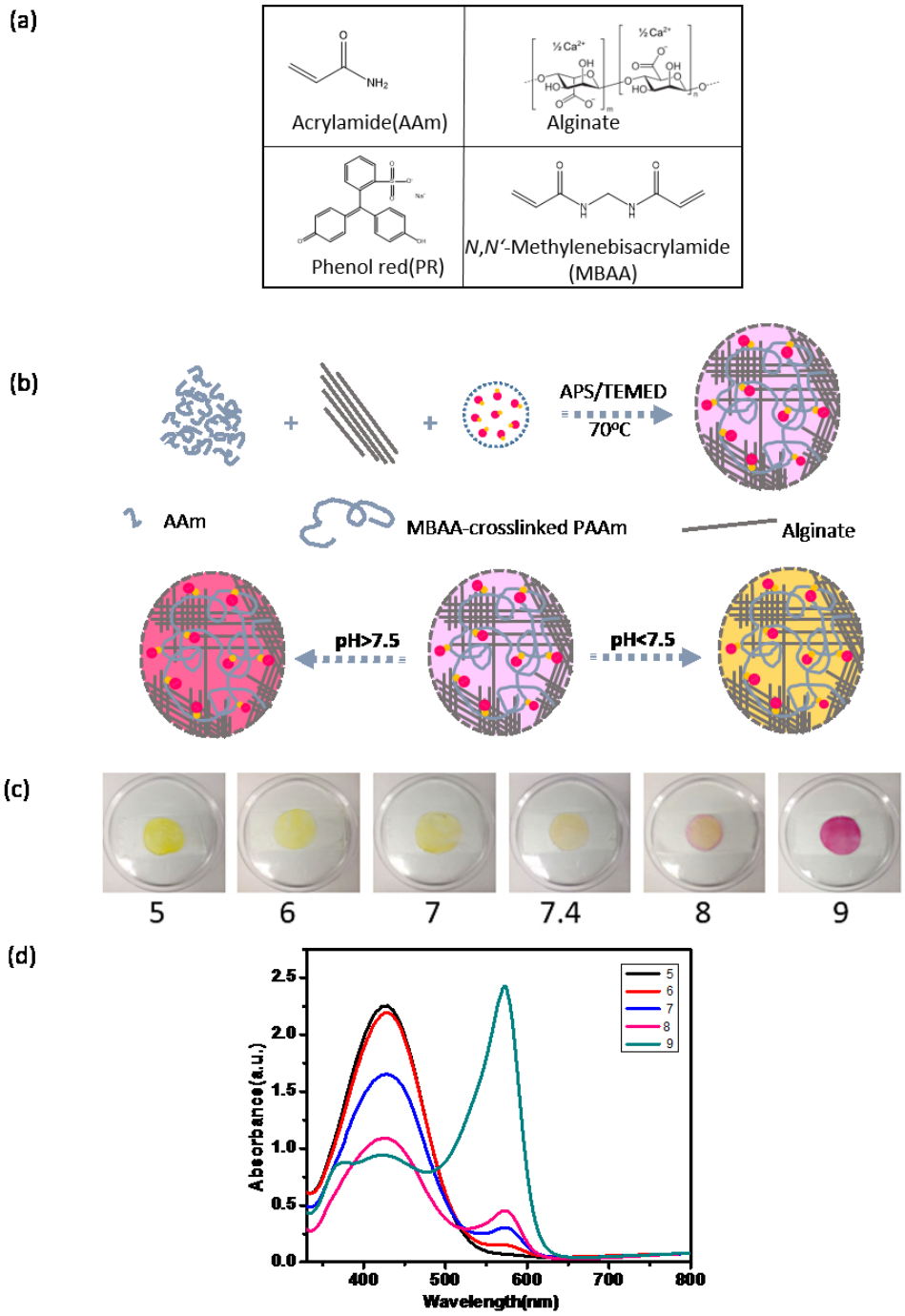

Figure 3.2 Preparation and characterization of P(AAm-MAPR)/alginate hydrogel dressings. (a) The chemical structures and the names of the monomers, the dye and the cross-linker used in the synthesis of the alginate/P(AAm-MAPR) hydrogel dressing. (b) Synthetic strategy and colorimetric transitions of the alginate/P(AAm-MAPR) hydrogel dressing. (c) Photographic images that captured the colorimetric transition of the hydrogel dressing in buffer solutions with pH values from 5 to 9 (from left to right). (d) UV-Vis absorption spectra of the hydrogel dressing while immersed in buffer solutions with pH values from 5 to 9.

3.3 Physical evaluation of hydrogel dressings as a function of P(AAm-MAPR) crosslinking density

The physical properties of the hydrogel dressing, including surface and interior morphologies, mechanical properties, swelling ratio, water vapor transmission rate, were evaluated for the P(AAm-MAPR) hydrogels with various crosslinking densities. Fig 3.3 (a) showed the surface (1-3) and cross-section (4-6) images of various hydrogels observed by SEM. The surface (1-3) did not show visible open pores but displayed a relatively smooth structure with tangled strands. A comparison between low (1) and high (3) crosslinking densities revealed that the network structure was denser in the higher crosslinking case, as evidenced by the appearance of increased entanglement of the strands. The interior structures of the hydrogels were visualized in the cross-sectional images in (4-6). Here, the hydrogel showed a highly porous honeycomb-like structure, which could be helpful for the supply of oxygen, the absorption of exudates, and the containing of large amount of water [75]. Increasing concentration of MBAA (crosslinker for P(AAm-MAPR) networks) resulted in the reduction of the averaged pore size; the average diameter of pores decreased from 80 μm to 40 μm finally to 20 μm as the MBAA concentration increased from 0.05% to 0.1% and to 0.15%.

Mechanical properties of the hydrogel wound dressing play a significant role in establishing the dressing's structural integrity during the application, which is a dominant factor to determine the target wound. Hydrogel dressings must be able to withstand the applied stress on the wound site, and must have high tolerance to swelling or motion-induced deformation to avoid breakage by exudate absorption and by patient's movements. The ductility was quantified by determining the elongation at break [76]. Fig 3.3 (b) showed the tensile stress-strain curves of the hydrogel dressings with the three crosslinking densities as used in Fig 3.3 (a). Young's moduli and

elongations at break values were obtained from the Fig 3.3 (b) and presented in Fig 3.3 (c). The results revealed that the hydrogel dressing with the medium crosslinking density had maximum Young's modulus of 0.55 MPa, whereas 0.2 MPa was observed in the high and the low crosslinking density cases. This demonstrated that increases in the chemical crosslinking of P(AAm-MAPR) networks or in the physical entanglement between the two networks did not guarantee the increases in the stiffness of the double network alginate/P(AAm-MAPR) hydrogel. Instead, a right amount of fluidity could optimize the dissipation of the applied stress by the alginate, which was a softer network with reversible ionic bonding, and this resulted in the enhancement of the mechanical strength [77]. Hence, medium crosslinking density (0.1wt% MBAA) provided the optimum condition among three crosslinking densities. The increase of MBAA concentration from 0.05 wt % to 0.15 wt % significantly increased the elongation at the break of the hydrogel from 80% to 686%. This was ascribed to the enhanced stretchability of the hydrogel originated from the fact that increased MBAA decreased the necessity of breaking non-reversible covalent bondings in the P(AAm-MAPR) network at a given strain level, resulting in detrimental breakage of the structure at lower elongation.

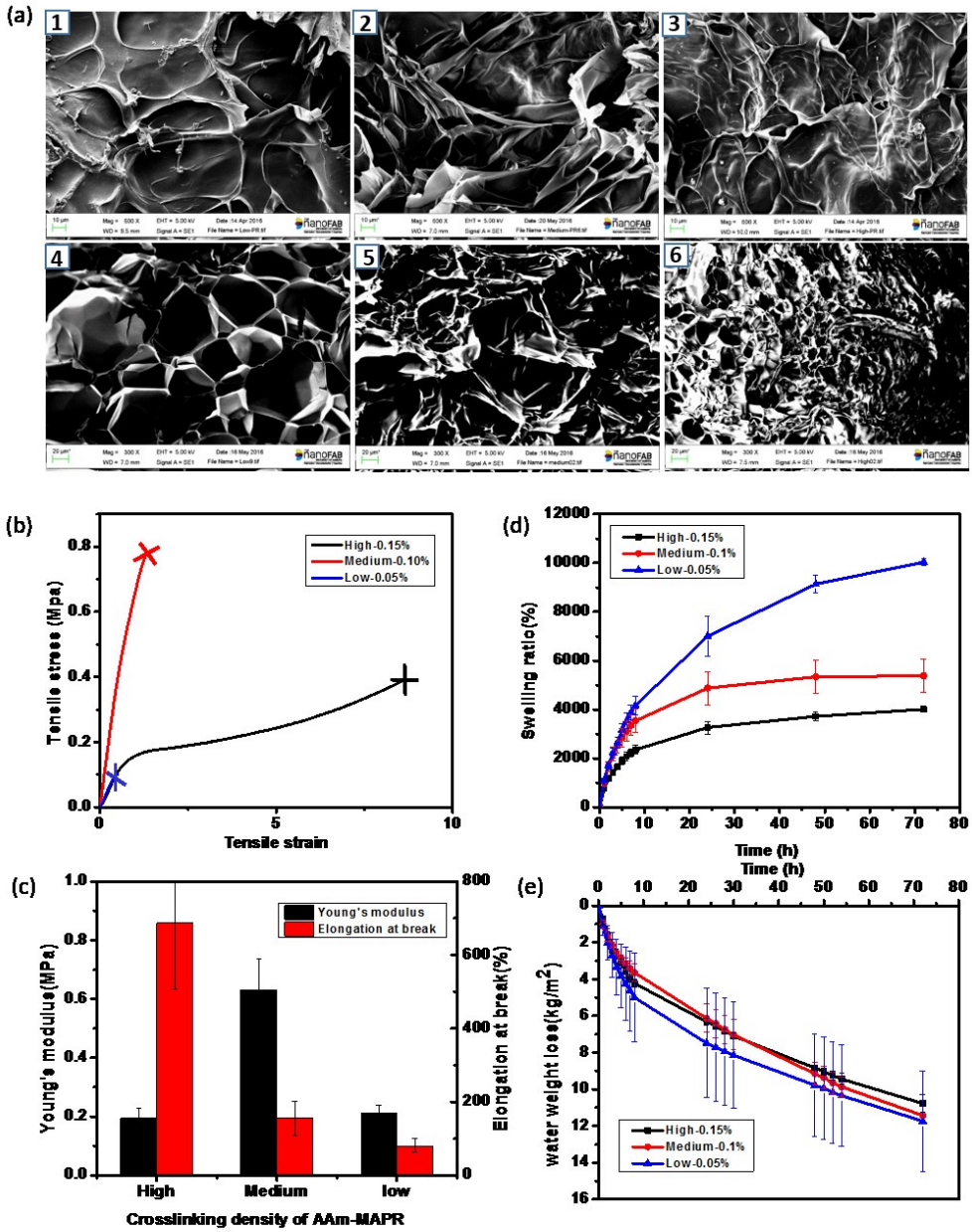

Figure 3.3 Evaluation of the physical properties of the hydrogel dressings as a function of crosslinking density of the P(AAm-MAPR) network. (a) SEM images of hydrogel dressing with the three crosslinking densities from the surface (1-3) and the cross-section views (4-6): 1 and 4 - high crosslinking density (0.15% MBAA concentration); 2 and 5 - medium crosslinking density (0.1 % MBAA concentration); 3 and 6 – low crosslinking density (0.05 % MBAA concentration). (b) Tensile stress – strain curves, (c) Young's modulus and elongation at break, (d) Swelling ratio and (e) Water vapor transmission rate of the hydrogel dressings with the three crosslinking densities.

A moist wound environment is important in modern therapy because it can promote the penetration of the substances that aid in healing process and protect wounds against bacterial invasion. The moisture in the dressing also enables a painless dressing removal without damage to the newly formed skin [78]. An ideal wound dressing is supposed to lock the exudate and maintain a proper moisture level during the healing process. Therefore, measurements of swelling ratio and water vapor transmission rate were performed and are presented in Figs 3.3 (d) and (e), respectively. Fig 3.3 (d) showed that the hydrogel dressings with the high and the medium crosslinking densities reached a near-equilibrium swelling after 24 h immersion in buffer solutions with physiological pH of 7.4 at 37 ^{o}C, whereas the sample with the low crosslinking density did not show a saturation up to 72 h, which was the longest duration of the current study. The equilibrium swelling ratio was in the range of 4020% -5043%. The water absorptivity and equilibrium water content of hydrogel dressing increased as the concentration of MBAA decreased, which was due to the decreased contraction stress that stemmed from the intrinsic stiffness of the hydrogel networks [7]. The high swelling ability of the hydrogel is preferable for wound dressing because such dressings can effectively protect the wound bed from exudate accumulation, thus reduce the necessity for frequent replacement [79].

Wound dressing should have proper water vapor transmission properties to develop a favorable environment for speedy healing. Therefore, water vapor transmission rate, which is a qualified form of the water vapor diffusion ability, is an important parameter for wound dressing materials [80]. According to the literature, the average WVTRs for normal skin, first degree burns, and granulating wounds are 204 ± 12, 279 ± 26, and 5138 ± 202 g/m^2/day, respectively [81]. WVTR of the dressing should be neither too low nor too high, since a low permeability may cause the accumulation of the exudates and result in the leakage, whereas a high permeability may lead to

excessive dehydration of the wound surface [7]. It has been suggested that the WTVR for a good wound dressing should be in the range of 2000 – 2500 g/m^2/day, which can maintain a proper moisture on the wound without dehydration [82]. The WVTR values of the hydrogel dressing with the three crosslinking densities are shown in Fig 3.3 (e). In the beginning 5 hrs, the weight loss was rather rapid and the trend was non-linear; linear slopes occurred between 10 and 72 hrs. The initial non-linearity could be ascribed to the transient period when the vapor molecules condensed on the surface and subsequently solubilized into the porous structure of the hydrogel. Once the transient period was over, the later-incoming water vapor molecules experienced a steady-state diffusion through the width of the film [83]. WVTR was determined from the linear portion of the graph; all of the three hydrogel dressings showed similar WVTR values of 2387 g/m^2/day, belonging to the range of 2000 – 2500 g/m^2/day. All the measurements demonstrated that alginate/P(AAm-MAPR) hydrogels prepared in our study were suitable materials for wound dressing application.

3.4 Investigation of mechanical properties under various calcium and water contents

Alginate-based dressings have a pharmacological function due to the action of calcium ions present in the dressing [84]. Calcium released through ion exchange with sodium in the wound exudates can effectively promote hemostasis during the first stage of wound healing [85]. In addition, calcium is the ionic crosslinking agent used in the alginate hydrogel formation, thus the increase of its content can strengthen the hydrogel's mechanical strength. Hence, hydrogel dressings at various calcium concentrations (0.01%, 0.1%, 0.3%, 0.5%) were prepared to study the effects of calcium concentrations on the mechanical properties. Figure 3.4 (a) shows the

tensile stress-strain curves of the hydrogel dressings with various Ca^{2+} concentrations. Figure 3.4 (b) shows the corresponding values of Young's moduli and elongations at break. With the increase of Ca^{2+} concentration from 0.01% to 0.1%, the Young's modulus was moderately increased from 0.39 MPa to 0.61 MPa, whereas the moduli values were nearly invariant at the higher concentration of 0.1% - 0.5%. It was also found that, from both Figs 3.4 (a) and (b), increasing calcium content resulted in a more stretchable hydrogel. With 5% Calcium content, the elongation at break of the hydrogel could be up to 250%. In summary, the Ca^{2+} concentration had a significant influence on the hydrogels' mechanical properties, especially on the elasticity.

Water content is important for hydrogel dressing because it provides a moist environment for the wound, which is a key factor for the wound healing. It also modulates the permeation of gases and ions to the wound site [86]. However, the swelling of the hydrogel dressing changes with time after the initial application on the wound according to the conditions of wound healing and to the ambient environment. The swelling conditions, especially the water contents in the hydrogel, dictate the mechanical strength of hydrogels. Therefore, we investigated the effect of swelling/drying conditions on the Young's moduli and elongations at break of the prepared hydrogel dressings. Fig 3.4 (c) shows the various swelling/drying conditions and resulting swelling ratio values. As shown in Fig 3.4 (d), the Young's modulus increased dramatically from 0.67 MPa to 155 Mpa as drying time increased from 1 hr to 3 hrs. The extremely high mechanical strength of the hydrogel for drying 3 hours could be attributed to the exceptionally low water content (i.e., swelling ratio of 63.1%) compared to the that of original dressings (251.5%) or other samples. In the case of swelling up to 3 hours, Young's modulus was in the range of 0.4 – 0.7 MPa without significant variations. The values of elongation at break showed rather scattered results. But in general, the elongation at break increased as the swelling ratio

became higher. After drying the hydrogel sample three hours and then swelling three hours, the Young's modulus was 2.7 times higher than that of the original one, while the elongation remained almost the same. This could possibly suggest that some irreversible internal structure change happened after the drying process, thus re-swelling the hydrogel for three hours may not recover the original modulus.

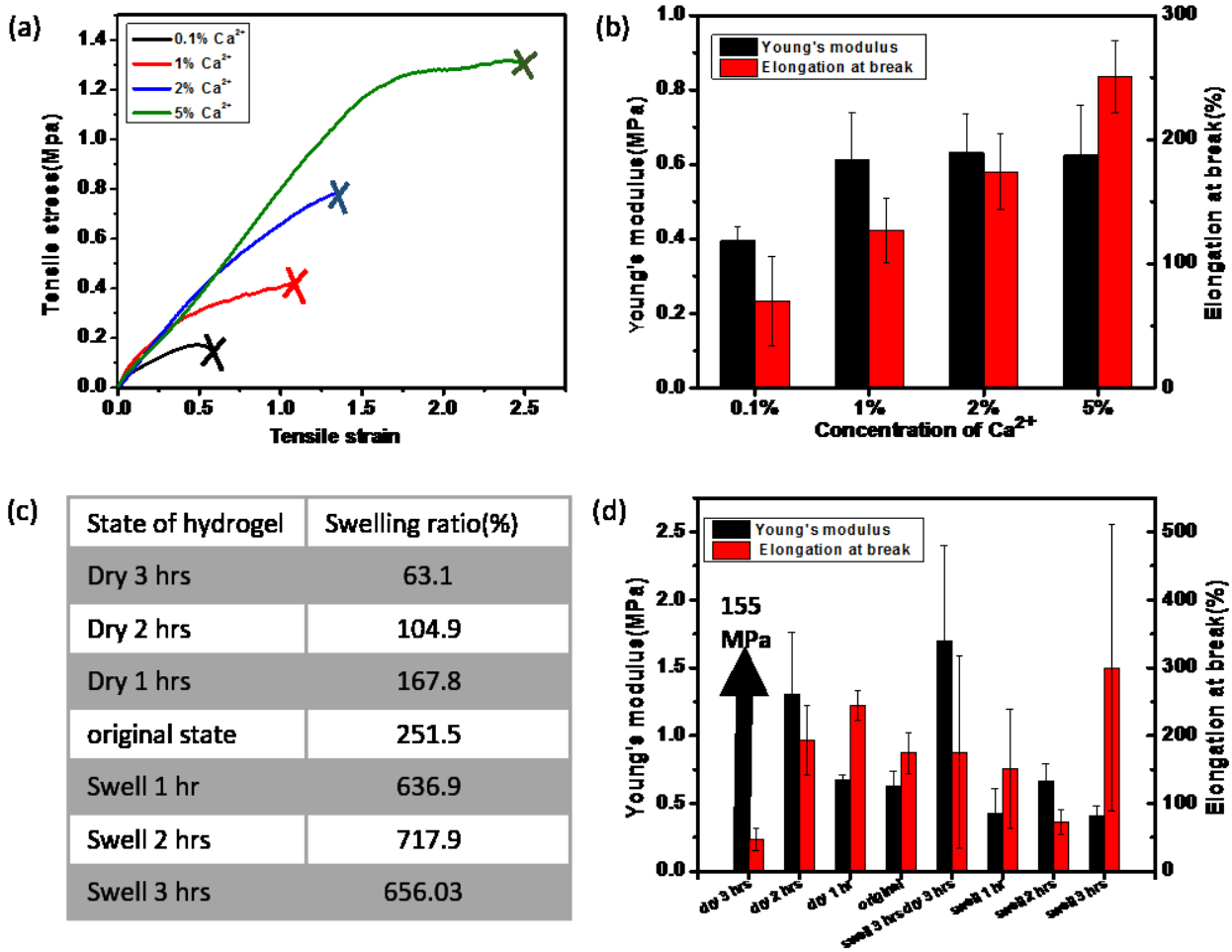

State of hydrogel	Swelling ratio(%)
Dry 3 hrs	63.1
Dry 2 hrs	104.9
Dry 1 hrs	167.8
original state	251.5
Swell 1 hr	636.9
Swell 2 hrs	717.9
Swell 3 hrs	656.03

Figure 3.4 Investigation of the mechanical properties as a function of Ca^{2+} concentrations (a, b) and time-dependant swelling/drying conditions (c, d). (a) Tensile stress-strain curves and (b) Young's modulus and elongation at break values with various calcium concentrations. (c) Swelling ratio and (d) Young's modulus and elongation at break values at various time-dependant swelling/drying conditions. All hydrogels have the MBAA concentration of 0.10%. The original state refers to the synthesis condition that hydrogel was vacuum dried in the oven for 2 hrs at 65 ^{o}C after dialysis of 3 days.

3.5 Leaching test

Dye leaching was evaluated by storing the hydrogel strips with 1cm × 2cm dimension in large amount of water for 7 days at room temperature. Water was changed daily to efficiently remove any unreacted monomers, including the dye molecules that did not participate in the copolymerization to form covalent bonding with the hydrogel network. The absorbance spectra of the hydrogel were recorded from day 0 (without leaching) to day 7 (leached for 7 days), and results are shown in Fig 3.5 (a). The absorbance at 568 nm as a function of the washing time was plotted in Fig 3.5 (b). As shown in both Fig 3.5 (a) and (b), the absorbance at 568 nm was greatly reduced from day 0 to day 2. This was partially ascribed to the loss of unmodified PR and unreacted MA-PR in the dialysis of the first two days. According to our swelling ratio test, hydrogels reached the equilibrium status of swelling within the three days. Hence, from day 3, all of the hydrogel strips were in equilibrium state and MA-PR concentration inside of the hydrogel remained the same. It can be observed that the absorbance was almost unchanged from day 3 to day 7, which means no loss of the dye was detected during this period. This demonstrated that the covalent attachment of the dye to hydrogel substrate could significantly prevent the leaching of the dye. It can be concluded that three days of dye leaching can prevent the potential damage on wound by the cytotoxicity of the untreated dye molecules.

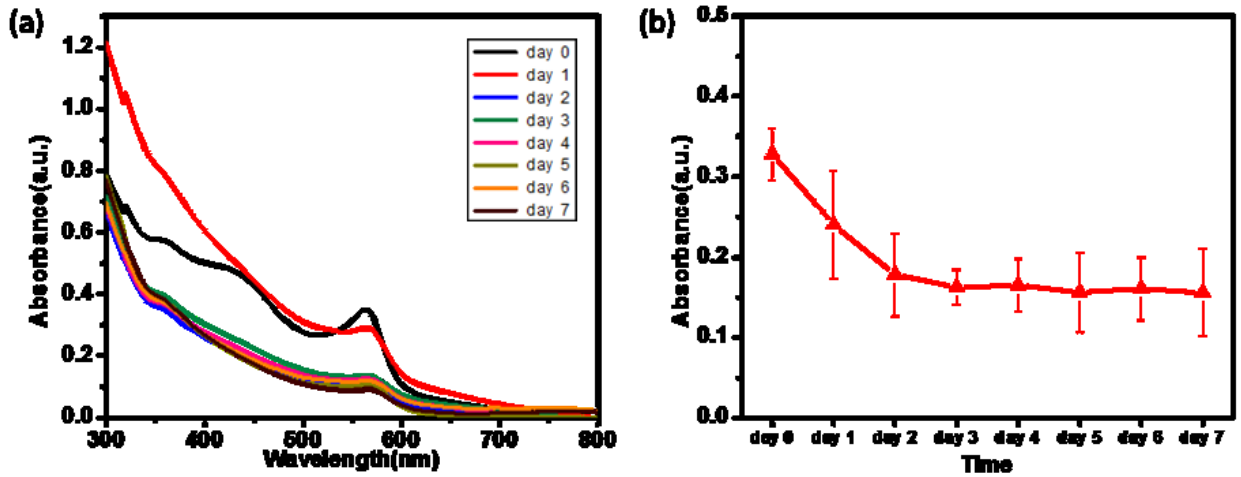

Figure 3.5 Leaching of the dye over 7 days of dialysis in deionized water. (a) UV-Vis absorbance spectra of the hydrogel from day 0 (without leaching) to day 7 (leached for 7 days). (b) Absorbance at 568 nm as a function of leaching time.

3.6 Conclusions

A series of pH indicating colorimetric alginate/P(AAm-MAPR) hydrogels were synthesized for potential wound dressing application. The pH indicator dye phenol red was successfully modified with methacrylate and subsequently copolymerized into the double network hydrogel matrix. This covalent attachment could prevent the dye from leaching out of the matrix. When immersed in buffer solutions with various pH values, the color of the hydrogel dressing underwent a transition from yellow (pH 5, 6 and 7) to bisque (7.4 and 8) and finally to red (pH 9), which matches the required pH range for the application to chronic or infected wounds. The prepared hydrogel dressings showed porous internal structures, excellent mechanical properties, high swelling ratio and appropriate water vapor transmission rate; these features indicated that the hydrogels were suitable for wound dressing applications. In addition, calcium content could significantly impact the Young's modulus and elongation at break of the hydrogel. In conclusion,

our alginate/P(AAm-MAPR) hydrogel could be used as wound dressing material that allowed monitoring the wound healing process by a simple colorimetric display.

Chapter 4. Medical Grade Silicone Adhesives: A Non-Irritative Solution for Electronic Patches on Skin

4.1 Introduction

Adhesives that are directly in contact with human skin have a long history; one famous example is Band-Aid®. The earliest skin adhesive material used in clinical applications was natural rubber based medical tapes, which were soon replaced by synthetic materials. Based on the choice of adhesive material, synthetic adhesives can also be used in non-medical applications, such as automobile decals and detachable labels. Pressure-sensitive adhesives (PSA), which form a bond when pressure is applied to join the adhesive with the substrate, was first introduced by Johnson & Johnson in 1899. More recent applications of the PSA include transdermal drug delivery systems and adhesives for skin mountable medical devices [87].

This chapter discusses the terminology used in the adhesive technology. The mechanism of adhesion and required characteristics of human skin adhesives are also reviewed in detail. Different classes of adhesive types are listed and described. Finally, testing methods to quantitatively characterize the adhesives are introduced.

4.1.1 Adhesion and tack

The two most commonly used terminologies in adhesives are 'adhesion' and 'tack'. Adhesion is an action or a process to stick two different substances together. Tack refers to the instantaneous level of adhesion when an adhesive is applied on a surface. In order to hold adhesives in

position, a high level of tack is needed. When applied to the skin, the adhesion of adhesives is at its maximum at the moment of application but gradually decreases due to transdermal water evaporation and skin desquamation.

There are some specific requirements for ideal adhesives for skin application. Adhesives must have sufficient initial tack to secure the position of adhering subject upon application, and then their stickiness should be adequate to hold the subject in position throughout the wearing time. Furthermore, the removal of adhesives should not cause trauma to the skin. The adhesives are also expected to be non-irritant, non-sensitising and residue-free [88].

4.1.2 Requirements of skin adhesives

4.1.2.1 Toxicological

In medical applications, skin adhesives must not be toxic; in other words, the adhesive must not provoke skin reactions. There are two major types of skin reactions – primary skin irritation (PSI) and skin sensitization. The former is categorized by the Primary Irritation Index (PII), while the latter one is measured with the Repeat Patch Insult (RPI) test. In the PSI test, reactions including redness and swelling are monitored while the adhesive is attached on the skin. In the RPI test, the adhesive is placed on and off the designated site of skin while periods of wash-out are allowed. Afterwards, the same adhesive is attached to a different site on the skin. Redness and swelling are monitored on both sites. An intermediate test is also required for RPI test. This intermediate test sticks the adhesive to the same site on the skin several times and then measures the redness and swelling.

It is noteworthy that PSI is observed upon the first application of adhesive on skin, whereas skin sensitization happens after multiple applications. The biochemical origin of PSI reactions is that chemicals in the adhesives induce stimulation of nerve endings, resulting in the painful feeling. Red and white blood cells that are brought to the site is a consequence of the vasodilation from the chemicals. Swelling of the skin originates from the extravasation of various cells. The biochemical origin of sensitization is far more complex. Two types of hypersensitivity exist: Immediate Type Hypersensitivity (ITH) and Delayed-Type Hypersensitivity (DTH). When redness, swelling and itching are observed within 2 hours, the reaction is classified as ITH, whereas DTH requires 24-72 hours of application to induce the reactions. DTH is believed to be the reason for most skin sensitizations. Skin sensitization is involved with the activation of immune system, whereas PSI is not. Therefore, PSI caused by adhesives can be acceptable for patients, but skin sensitization should not be tolerated.

Skin adhesives used in bandages, transdermal systems and electromyogram (EMG) devices must pass the requirements of the PSI test and the sensitization test. These tests are implemented on animals first, such as pigs and rabbits. Once proven to be safe, clinical tests on humans can be considered. The skin irritation potential of chemicals is summarized as the primary irritation index (PII). The PII is calculated from the grade of redness and swelling [89].The acceptable index in the PSI test is less than 3.0. Sensitization potential is defined as the percentage of animals showing the adverse reaction after 24 or 48 hours [90]. If 0% to 8% of tested animals exhibit such reaction, it is weak sensitization; if the percentage is as high as 81% to 100%, it can be regarded as extreme sensitization.

Cytotoxicity is also an important factor to determine the applicability of adhesives. The degree of cytotoxicity is determined by systemically injecting the water soluble components of

adhesives into the dermal site of the tested animals, such as rabbits and mice. The test results are rated by a U.S. Pharmacopeial Convention (USP, a scientific nonprofit organization that are enforceable in the United States by the Food and Drug Administration to set standards for the identity, strength, quality, and purity of medicines, food ingredients and so on [91]) classification, the higher of which means the material is more benign [87].

4.1.2.2 Adhesion requirements

Adhesion requirements vary widely based on specificity of each application. For bandages, the adhesive's duration time, ranging from a few hours to one or two weeks, may be accepted. But this may not be crucial in most cases because most people change the bandage daily, or just after a shower. Besides, the backing material in a bandage is breathable, which is good for long term adhesion. In other applications like transdermal drug delivery systems, adhesives should be durable for at least 24 hours. For surface EMG devices, adhesives are also expected to be sticky on skin for one to three days [87].

4.1.3 Mechanisms of adhesion

There are four theories to explain mechanisms of adhesion that have been proposed: mechanical interlocking theory, diffusion theory, electronic theory, and adsorption theory.

4.1.3.1 Mechanical interlocking theory

Intrinsic adhesion refers to the direct molecular forces of attraction between the adhesive and the substrate. It is mainly used to distinguish the measured adhesion, such as measured strength or

toughness of the adhesive joint [92]. In this theory, the intrinsic adhesion is derived from mechanical interlocking between the adhesives and the irregularities of the substrate surface. The general applicability of this theory is challenged by the good adhesion between two smooth surfaces, where interlocking is difficult to form. Nevertheless, mechanical interlocking has proved to be a dominant mechanism in many cases [93].

The adhesion between polymers and textiles is a good example. In Borroff and Wake's experiment [94] to elucidate the mechanism of the adhesion between a rubber and an uncoated fabric, the most dominant mechanism of adhesion was the penetration of the protruding fiber ends into the rubber. When the rubber/textile mixture was compressed, the length of the penetrated fiber was sufficient to generate shearing force to prevent disjoining of the two materials. This force exceeded the breaking strength of the fiber so that the textile could remain sticky on rubber. The adhesion at the rubber/textile interface was attributed to the covalent or van der Waals bonding. If the textile is woven from continuous filament yarn, the fiber ends are removed, which means that the mechanical interlocking will no longer exist. Examples of such textiles include rayon and nylon. In this case, some pre-treatments need to be performed on the textile to increase the intrinsic adhesion. Chemical treatment by isocyanates or resorcinolformaldehyde are typically implemented [95].

Wake [96] suggested a model to quantitatively describe the measured joint strength that quantifies the adhesion between two surfaces. He concluded that the mechanical component essential to the performance of the joint was of great importance for the joint strength of adhesives. However, this type of component could not suffice the sole mechanism, thus the surface component beneficial for adhesion was joined. This model demonstrated that the substrate should have both rough surface topography and interfacial chemical interactions to

generate high joint strength. The enhancement of the joint strength may be achieved by increasing roughness of the substrate.

Although it is clear that mechanical interlocking increases with roughness and is the dominant mechanism in certain circumstances, the frequently observed increase of joint strength resulting from increasing surface roughness may be attributable to other mechanisms [93]. These mechanisms will be introduced in the next three subsections.

4.1.3.2 Diffusion theory

Voyutskii [97] proposed the diffusion theory of adhesion, which stated that the intrinsic adhesion of polymers to themselves (autohesion), and to each other (interfusion), resulted from mutual diffusion of polymer molecules across the interfaces. To allow this mechanism to be significant, the polymer molecules should be sufficiently mobile and mutually soluble. In the solubility model, similar solubility parameters between polymers implies that they are mutually soluble. The solubility parameter δ can be defined as

$$\delta = \frac{\Delta H^V - RT^{\frac{1}{2}}}{V}$$ [98],

where ΔH^V is the molar heat of vapourization, R is the gas constant, T is the temperature (K), and V is the molar volume.

Voyutskii found that the measured joint strength is a function of the retention time at contact, temperature, polymer type, molecular weight, and viscosity. Since they are important parameters for diffusion, he argued that the adhesion was a result of diffusion. However, it was also pointed

out that the dependence of joint strength on these parameters could be partially attributed to the kinetics of wetting, or energy dissipation [99].

As for autohesion, theoretical predictions and experimental results agree that autohesion is a function of a polymer's molecular weight and time of contact. Campion [100] has shown that a polymer's molecular structure dictated the amount of cavities between different chains, which directly impacted the diffusion rate across the interface. Based on the model, the degree of autohesion of various elastomers could be deterministically predicted.

Interdiffusion is extremely important in the solvent-welding of plastics, where the solvent temporarily promotes the adhesion of plastic component. The solvent should strongly plasticise the surface of polymer to increase the free volume so that the mobility of polymer chain in the interface can increase. Structural restriction on polymer chain movements like crosslinking and crystal formation may be detrimental for interfusion.

In the examples mentioned above, diffusion significantly contributed to the intrinsic adhesion. However, when the solubility parameters of materials are not close, or when polymers are highly crosslinked or crystalline, the effect of interdiffusion becomes negligible [93].

4.1.3.3 Electronic theory

Different electronic band structures between the adhesive and substrate may result in electron transfer at the interface by balancing Fermi levels. The band structure alignment can subsequently form a double layer of electrical charge. Deryaguin et al. [101] suggested that the electrostatic forces arising from the interfacial electric charges may contribute greatly to the intrinsic adhesion.

In Deryaguin's theory, the interface between the adhesive and the substrate system can be treated as a capacitor. When two different materials are in contact, the capacitor will get charged. Discharge occurs when the capacitor separates due to interface rupture. Adhesion can be generated by these attractive forces in the electrical double layer. Deryaguin measured adhesion from peel tests, and then equated the measured work of adhesion with the calculated electrical energy using the capacitor model. Good agreement was found between these two quantities. However, this calculation was not very reasonable because the majority of the measured work of adhesion was dissipated through materials' viscoelastic responses. The viscoelastic energy should be deducted to qualify the electrical energy precisely.

Graf Von Harrach and Chapman [102] have confirmed the electrostatic contribution to the work of adhesion by measuring charge densities on a glass insulator substrate coated with gold, silver, or copper. The influence of an electrostatic double layer was also demonstrated at the interface between Zr-coated gold spheres and CdS single crystal substrates. They used a centrifugal technique, where the adhesive system was illuminated to measure the adhesive force by measuring the intensity of photoluminescence [103].

Most of research results were produced from electronic properties of pure materials. However, most metals are covered with an oxide layer, which possess its own electronic band structure. In practice, this complicates the effect of the electron transfer mechanism [93].

4.1.3.4 Adsorption theory

The adsorption theory is the most widely accepted theory. The theory proposes that the intimate intermolecular contact in the two materials provides surface forces to create adherence. Van der

Waals force is the most common type among the surface forces, which is also called secondary bonding. In addition, ionic, covalent and metallic bondings may also exist across the interfaces due to the possible occurrence of chemisorption. These bondings are referred to primary bondings [104, 105].

Huntsberger [106] has calculated the attractive forces between two planar materials. The force was solely from van der Waals force. According to the calculation, the attractive force reached 100 MPa even if the two surfaces were separated by one nanometer. However, this result was much higher than the experimentally measured joint strength. It could be explained by the voids, cracks, defects, or other geometric features present in joint at the interface between the two surfaces, which drastically reduced the effective contact area. These features also worked as stress raisers, causing premature rupture of the joint when the stress was far lower than the theoretical value. Even so, it still indicated that high joint strengths originated from the intrinsic adhesion that was attributable to the van der Waals force interactions.

It has also been suggested that acid-base interactions at the interface could contribute to the intrinsic adhesion forces. Bolger and Michaels' group [107] studied the effect of the acid-base interactions, resulting from the hydroxylated metal oxide substrates and organic functional groups provided by the adhesive.

Despite the evidence that the secondary bonding forces can critically contribute to the joint strength, many adhesion researchers still believe that strong primary bonding is a necessary requirement for environmentally stable interfaces. The use of complicated, surface-specific, analytical techniques like Laser-Raman spectroscopy [108], X-ray photoelectron spectroscopy [109] and secondary-ion mass spectroscopy [110] have provided direct evidence that primary bonding played a significant part in the contribution to the intrinsic adhesion.

Adhesion promotors and coupling agents have been employed to enhance the joint strength and its environmental resistance. The most common type is a silane coupling agent, which is extensively used as a surface finish on glass fibers in polymeric composite, as an additive in adhesive formulations, and as a primer in substrate prior to adhesive bonding. It is generally accepted that formation of strong, primary interfacial bonds helps to increase the joint durability against adverse effect originating from environment. For the polysiloxane-substrate surface, it is Si-O-substrate bond [93].

4.1.4 Adhesive types

Adhesives are broadly classified into pressure sensitive type and structural type. Most skin adhesives belong to the pressure sensitive category. Pressure sensitive adhesives can be made either permanent or removable. Examples of permanent applications include safety labels for power equipment, foil tape for heating, and sound/vibration damping films. These permanent adhesives have high adhesion strength as well as high performance, such as heavy load bearing ability even at elevated temperatures.

Removable adhesives form a temporary bond at the interface. They are required to leave no residue on the substrate after removal. They are usually applied as surface protecting films, bookmark, notepapers, wound dressings, electrocardiogram electrodes, and transdermal drug patches. The adhesion of these adhesives is generally low, and their weight supporting capacity is also weak.

4.1.4.1 Acrylic adhesives

Acrylic adhesives are able to provide a secure anchorage on the skin, but they are difficult to remove. Besides, they have a propensity to leave residue on skin and a tendency to cause skin trauma after removal [111]. Some of them even result in irritation reactions [112].

When adhesives are applied to skin, it is mandated that the manufacturer must perform PSI (irritation) and PRI (sensitization) evaluations. Cytotoxicity testing can also be performed but not mandatory. For long-term applications such as bandages or medical tapes, cumulative irritation studies may need to be carried out by repeatedly applying the acrylic adhesives at the same site [87].

4.1.4.2 Rubber-based adhesives

Traditional rubber-based adhesives were composed of natural rubber latex; currently, synthetic rubbers are used. They are mainly applied in surgical tapes and bandages. The adhesion of these rubber adhesives is weak, which results in movement of the adhesive on the skin over time. There are also concerns about skin stripping upon removal, especially in the case of multiple uses. Due to their low permeability to gas, these adhesives may leave residue on the surface or cause skin irritation [88].

4.1.4.3 Polyurethane adhesives

Polyurethane adhesives are not widely used for skin applications. They have attracted attention because properties of polyurethane films are suitable for dressing applications. However, the use of these adhesives may cause skin stripping [111] and maceration problems [113].

4.1.4.4 Soft silicone adhesives

Soft silicone adhesives are also known as micro-adherents because they are able to create large intimate contact area on the skin, where the surface topography is extremely uneven. The tackiness of these adhesives may not decay or increase over time, whereas the strength of adhesion is adequate for skin application [88]. Besides, silicones are inert, non-toxic, and not sensitising [114].

Some clinical research has evaluated the effects of silicone adhesives on the periwound skin after repeated applications and removals. Results reveal that soft silicone adhesives cause less damage to the stratum corneum when compared to the acrylic and the polyurethane adhesives [111, 115, 116]. This was further examined by scanning electron microscopy (SEM). Two adhesive types, the acrylic adhesive and the silicone adhesive, were attached to the inner forearm of a healthy volunteer for 4 hours. After this period of time, they were removed and analysed under microscope. Obtained SEM images are illustrated in Fig 4.1. The acrylic adhesive was found to remove many epidermal cells after removal, while soft silicone adhesive was clean and smooth [88].

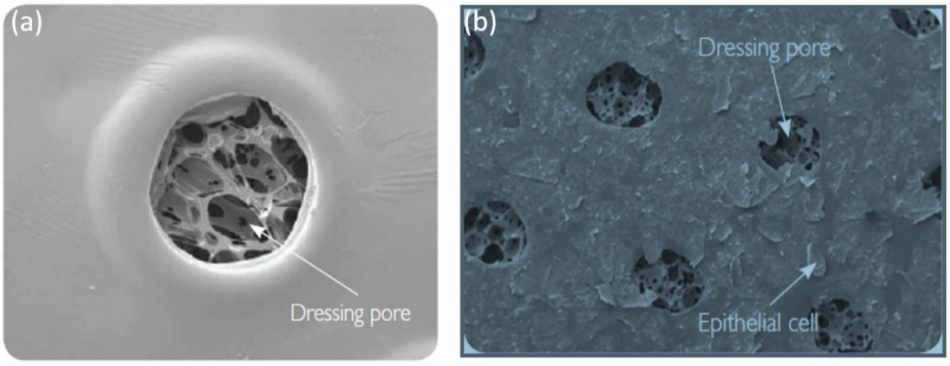

Figure 4.1 SEM images of (a) silicone adhesive and (b) acrylic adhesive after removal. Reproduced with permission from [88].

4.1.4.5 Cyanoacrylate adhesives

Cyanoacrylates are liquid and able to form high strength bonds to the skin when exposed to moisture. As a consequence, they are mainly applied as biological glues and tissue adhesives. More recent applications include the treatment of skin tears [117] and skin protectants [118] .

4.1.5 Testing of skin adhesive

The testing methods of skin adhesives can be divided into two broad categories: one is related to adhesive performance; the other one is associated with material properties. Examples of the former type are tack test and peel test. The latter one contains viscoelastic measurements, such as creep and dynamic-mechanical analysis.

4.1.5.1 Tacking test

The most reliable method to determine tack is probe tack measurement developed by Hammond [87]. It has already been commercialized as a Polyken Probe Tack tester. Tack is dependent on surface roughness and material properties of the substrate that the adhesive is attached to. The result of the test is influenced by contact time, contact pressure, and delamination rate.

The tack is a short term measurement of skin adhesion, which only demonstrates the initial tendency to stick to skin. Therefore, it is difficult to relate the tack to the long-term wearability. Minimum tack value can be set for all types of skin adhesives.

There are a series of procedures to follow for a tack test. Firstly, evaluate tack as a function of contact time, pressure and rate of withdrawal and estimate a number or range for these parameters. Then set parameters for the tack test; if results are not reproducible, establish another

set of conditions to obtain reproducible results. Use an adhesive that does not attach to skin as a negative control to evaluate the candidate adhesive for minimum acceptable tack. Apply a quick application and removal in this process. Finally, the maximum acceptable tack is defined at the point where adverse skin reactions occur upon removal. A quick application and removal is also required.

4.1.5.2 Peel adhesion test

Peel adhesion test is another method that needs to be standardized for each given application. It depends on contact pressure, contact time, the property of substrate, peel angle, and the withdrawal speed. The peel adhesion measurement is very different from the tack measurement because tack indicates the adhesiveness of application, while peel indicates the ease of removal. In addition, peel adhesion test can produce distinctive information under various conditions, including humidity and temperature.

Similar to the tack test, peel adhesion test also has points to be considered carefully; for example, its value is influenced by the properties of substrates, the rates of measurement, and the viscoelasticity of the adhesive.

4.1.5.3 Dynamic mechanical analysis test

Dynamic mechanical analysis can be used to measure the time-dependant viscoelastic behavior of skin adhesives. In the dynamic mechanical test, a disc-shaped sample is made. Here, a sinusoidal load in shear mode is applied on the one end of sample, and the applied stress can be measured by a stress transducer. At the other end of the sample, a strain transducer measures the

changes in length that results from the applied strain. The temperature of the sample chamber is usually controlled to be isothermal or ramped at a programmed rate [119]. The test output is complex modulus G*, which is composed of storage and loss components, as a function of frequency,

$G^* = G' + iG''$ [120].

The dynamic mechanical properties have been related to tack and peel. These relations are mostly empirical. The relation is established for polymer/tackifier blends but not for the acrylate family. Dynamic mechanical adhesion can be considered as a combination of the bonding process and the debonding process. The bonding process relates to relatively long times or small frequencies, while the debonding process relates to short time or high frequencies. Therefore, the moduli measured at low and high frequencies can be correlated to the measured tack and peel, respectively.

Dynamic mechanical measurements have been mainly applied in monitoring lot-to-lot variability or in validating mixing process of adhesives. The latter case is usually required in pharmaceutical product development [87].

4.1.5.4 Creep compliance

Creep compliance is a viscoelastic measurement that has great importance in evaluating the long term application on the skin. Here, if the material has a high tendency to creep, adhesives may ooze out of the backing. This exposed adhesive can pick up lint and stick to clothing. It also results in unattractive appearance as well as problems in storage and unwinding. Therefore, the

low creep compliance is highly recommended. But too low creep compliance usually relates to the loss of peel and tack, thus generally considered as not acceptable.

The creep compliance is measured by a controlled stress rheometer, in which the adhesive is pressed between parallel plates and heated to the desired temperature [87].

4.1.6 Summary

An ideal adhesive should not induce skin reactions, which means it must pass the PSI and sensitization tests. Adhesion requirement varies widely from several hours to a few weeks according to the applications, but adhesives should have appropriate tack and sustained adhesion throughout the duration. Four main mechanisms of adhesion, including mechanical interlocking theory, diffusion theory, electronic theory and absorption theory, are introduced in this chapter. A number of important adhesives are also listed, among which silicone adhesives are by far the most reusable and repeatedly removable. Performance evaluation is also important for adhesives. There are two broad testing categories: one is related to adhesive performance, such as tack and peel, and the other one is associated with material properties including dynamical mechanical analysis test and creep compliance test. To define a good skin adhesive, a combination of several testing methods to explore multiple aspects of properties will be necessary.

4.2 Objectives

Sensors to detect surface electromyography (sEMG) signals have been widely used by researchers and clinicians measuring electrical signals from muscle movements. These sEMG sensors are interfaced with human skin using single- or double-sided adhesives. Acrylic adhesives are the most commonly used and commercially available due to their strong tackiness

and low cost. However, they are not reusable, difficult to remove and easy to cause skin stripping. In addition, they have a tendency to leave residue on skin.

Here, we tested several commercial medical grade silicones as non-irritative alternatives to acrylic adhesives. The silicone adhesives were tacky, non-toxic, non-irritative, and residue-free after removal. Moreover, the silicone adhesives were easily washable and allowed multiple cycles of attach/detach; these advantages rendered the material to be an ideal solution for prolonged use of the electronic patch. Quantitative analysis on the adhesive performance, including peel strength, reusability and durability, were performed in this research.

4.3 Fabrication of silicone-based adhesives

4.3.1 Materials

Silbione 4717, Silbione 4624, and Silpuran gel were supplied by Bluestar Silicones (New Jersey, USA). Blue fabric was supported by our collaborator in the Department of Human Ecology, Mary Glasper. Pig skin was purchased from Lucky 97 Supermarket (Edmonton, Canada) and used to mimic human skin. Sunlight detergent and standard isopropyl alcohol swab were obtained from Shoppers Drug Mart (Edmonton, Canada). Clear Surgical Tape® (Dynarex, New York, USA), Nexcare Sensitive Skin Tape® (3M, Minnesota, USA), Band-Aid® (Johnson & Johnson, New Jersey, USA), Reusable Self Adhesive® (medical pad) and original Acrylic Pad® were purchased from Amazon in Canada. Bioflex 100P®, RX 1423®, Scapa soft pro 6054®, Scapa RX 1383S®, Scapa RX 1309S®, Scapa RX 1308S®, and Scapa RX 7435® were obtained from Scapa company (Connecticut, USA).

4.3.2 Fabrication of Silbione 4717, Silbione 4624 and Silpuran pads.

All of these silicone gels are two components, room temperature vulcanizing elastomers that crosslink at room temperature by polyaddition reaction. They were applied onto adhesive pads to achieve a thickness of 640- 740 µm. General fabrication procedures were as follows: The blue fabric was cut into a rectangular shape with a dimension of 50 mm × 30 mm by a Scan and Cut machine (Brother ScanNcut, Québec, Canada) and used as backing materials. First, part A and part B of the silicone gel were mixed well by hand with a 1:1 weight ratio and placed in a vacuum chamber to de-gas for 30 mins to eliminate any entrapped air. Afterwards 1- 1.2 g gel mixture was spread evenly on the cut fabric with a spoon and left at the room temperature for one day to be cured. The thickness of the adhesive pad was 640 µm, as measured by a caliper. In addition, Silbione 4717 adhesive pads with two different thickness range were also prepared. Here, 0.6-0.7 g and 2-2.2 g gel mixture were used to obtain adhesive layers with thicknesses of 240-340 µm and 1240 -1340 µm, respectively.

4.3.3 Peel strength analysis of the fabricated adhesive pads and commercial adhesive pads

A 90° peel test was conducted on pig skin to determine the peel strength of the fabricated adhesive pads and commercial adhesive pads (Clear Surgical Tape®, Nexcare Sensitive Skin Tape®, Band-Aid®, Reusable Self Adhesive® (medical pad) and original Acrylic Pad®) using the Instron 5943 with a 1 kN load cell. The pig skin was secured to a platform, and the adhesive pad was then placed on the pig skin. The long tail of the adhesive pad was secured in a set of upper clamps. The adhesive pad was peeled off mechanically the pig skin at a speed of 10 mm min^{-1}. The average peel strength was calculated by measuring the average load of the peel test and

dividing it by the width of the bonded pad. Each test was repeated three times to obtain an average peel strength.

4.3.4 Aging test of the fabricated adhesive pads

Silbione 4717 adhesive pads with thickness of 640 μm were chosen to perform an aging test over a 7-day period. During 7 days, adhesive pads were kept in petri dishes at room temperature. They were removed from the petri dish once a day and subjected to a peel test. The peel strength was measured using the above mentioned peel test method from day 1 (the first day after fabrication of the pad) to day 7 (the 7th day after fabrication of the pad).

4.3.5 Reusability test of the Silbione 4717 adhesive pads

Reusability of the Silbione 4717 adhesive pads was evaluated by washing test and wiping test. Washing test and wiping test can also be compared to determine a better cleaning method for patients. In the washing test, warm soapy water made from the dish detergent was used to clean the adhesive pad after each attachment to the pig skin. Four different washing times were compared in this test, which were 5, 10, 20 and 40 seconds. After each wash, the adhesive pads were dried by compressive air. For each washing condition, peel tests were performed after 1 adhesion/debonding cycle, 5 adhesion/debonding cycles, 10 adhesion/debonding cycles and 20 adhesion/debonding cycles.

In the wiping test, adhesives pads were cleaned by a standard isopropyl alcohol swab. Similarly, four different wipe numbers for each clean were compared. They were 0 wipe (no cleaning), 1 wipe, 5 wipes and 10 wipes in one adhesion/debonding cycle. For each wipe

number, peel tests were performed after 1 adhesion/debonding cycle, 5 adhesion/debonding cycles, 10 adhesion/debonding cycles and 20 adhesion/debonding cycles.

4.3.6 Peel strength analysis of different commercial adhesives used for sEMG device

Seven commercial adhesives used for sEMG applications, including Bioflex 100P®, RX 1423®, Scapa soft pro 6054®, Scapa RX 1383S®, Scapa RX 1309S®, Scapa RX 1308S®, and Scapa RX 7435®, were evaluated by peel test. Their peel strengths were determined using the same method mentioned in section 4.3.3.

4.3.7 Weight loading test of Scapa RX 1383 S adhesives system

Based on the results of the previous studies, the Scapa RX 1383 S® adhesive was found to have the best adhesion and peel strength. Therefore, Scapa RX 1383 S® adhesive was subjected to a weight loading test to evaluate its performance and to determine the mode of failure for each of weights. The experimental set up was shown in Fig 4.2. The polypropylene bar on top was applied to simulate skin because its surface energy is around 29 mJ/m^2, which is close to human skin's surface energy of 25 mJ/m^2. Silicone adhesive faced upwards towards the polypropylene surface. Various stainless steel weights (28 g, 46 g) that represents sEMG devices were attached to the acrylic side of the adhesive. A camera was used to entire test and video can be used to determine failure time for each of the weights.

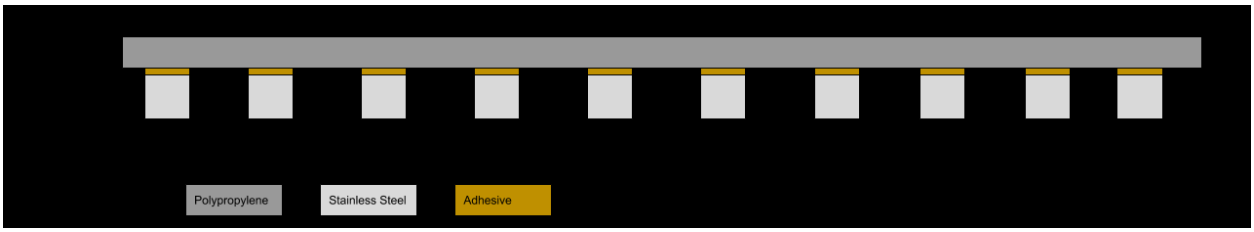

Figure 4.2 Experimental set up for a weight loading test of Scapa RX 1383 S® adhesives.

Chapter 5. Results and discussion of Silicone Skin Adhesives

5.1 Fabrication and characterization of silicone adhesive pads

The Silbione skin adhesives are two-part (part A is silicone gel and part B is platinum catalyst), platinum catalyzed silicone gel elastomers that crosslink at the room temperature by polyaddition reaction. The polymerization can be accelerated by heat [121]. A series of adhesive pads were fabricated. The blue fabric, which was composed of 85% polycotton and 15% cotton, was used as a backing material. Peel strength results of three silicone adhesives, Silbione 4717, Silbione 4624 and Silpuran, with thicknesses between 640 -740 μm, were compared. As shown in Fig 5.1 (a), all adhesive pads displayed clinically acceptable peel strength, but the mean strength for Silbione 4717 was significantly greater than those of Silbione 4624 and Silpuran. Hence Silbione 4717 was selected as the raw material to fabricate adhesive pads for sEMG devices. In order to determine the optimum thickness for Silbione 4717 adhesive, two other thickness ranges, 240-340 μm and 1240-1340 μm, were also evaluated as illustrated in Fig 5.1 (b). As thickness increased, peel strength was improved, but the thicker silicone layer (1240-1340 μm) tended to leave residue on skin. In summary, 640 -740 μm was the best thickness of the adhesive layer, as evidenced by appropriate peel strength and residue-free property.

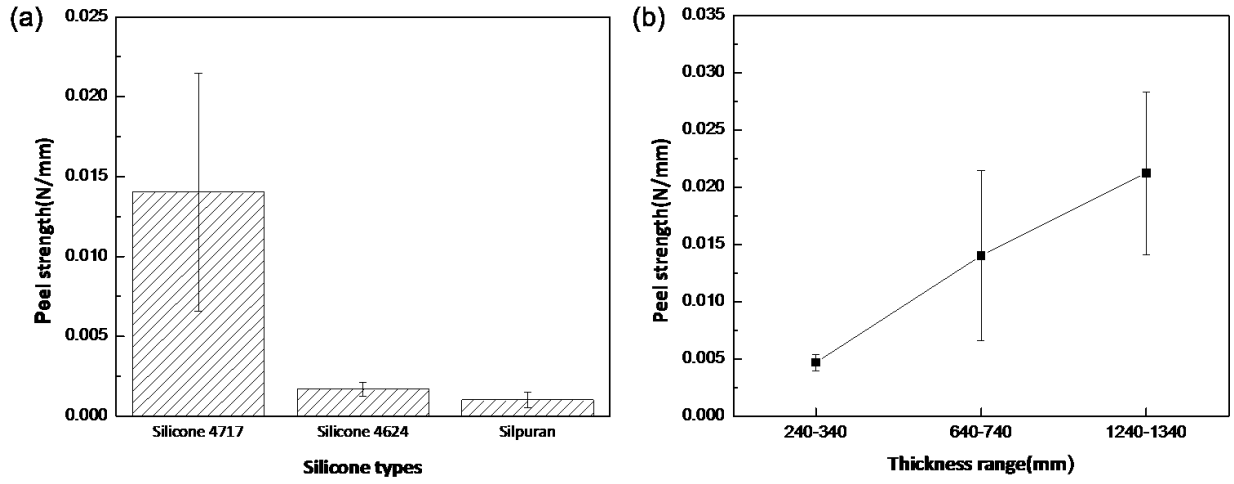

Figure 5.1 (a). Peel strength of three different commercial medical grade silicones at the thickness range between 600~800 μm. (b). Peel strength of Silbione 4717 at three different thickness ranges.

5.2 Comparison of Silbione 4717 and various skin adhesive products

The peel strength of Silbione 4717 adhesives with the optimized thickness was compared with those of adhesive products available in the market, including Clear Surgical Tape®, Nexcare Sensitive Skin Tape®, Band-Aid®, Reusable Self Adhesive® (medical pad) and original Acrylic Pad®. As shown in Fig 5.2, Silbione 4717 displayed an average peel strength that was significantly greater than those of Clear Surgical Tape®, Nexcare Sensitive Skin Tape®, Band-Aid®, and original Acrylic Pad®. Reusable Self Adhesive® (medical pad) was coated with long lasting reliable gel, thus possessing high tackiness on the skin. When compared with this highly sticky adhesive, the peel strength of Silbione was slightly higher, which demonstrated that the custom-made adhesive pad had a rather strong adhesion to the skin.

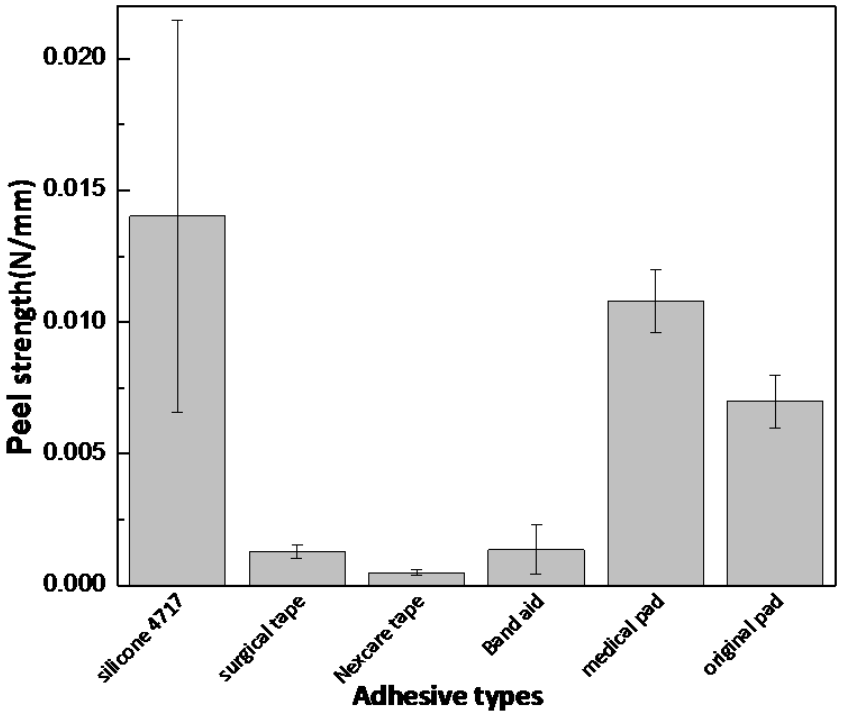

Figure 5.2 Peel strength of Silbione 4717 and its comparison against various commercial skin adhesive products.

Table 1 summarised the product information of the five commercial adhesives in Fig 5.2, including product features, target applications and functionalities. All of these adhesives are flexible, comfortable to use and possess good adhesion. Their main applications are either as wound dressing materials or sEMG patches.

Table 1. Summary of product information for five commercial adhesives

Product name	Clear Surgical Tape	Sensitive Skin Tape	Band Aid	Reusable Carbon Electrode Pads	Reusable Self Adhesive
Photo		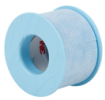			
Manufacturer	Dynarex	Nexcare (3M)	Johnson & Johnson	Easy@ Home Medical	Lemonbest
Product features	•Stretches and conforms to body contours •Superior adhesion •Highly porous	•Breathable •Conformable •Easy Tear •Water Resistant •Self-Adhering	•Extra tough durable •stretchable •comfortable	•Reusable •No Irritating to skin •Flexible •Compatible	•reusable •soft •flexible •effective
Peel strength (N/mm)	0.0013	0.0005	0.0014	0.0108	N/A
Target	hold the bandage or dressing on the skin	Fragile or sensitive skin	Small wound	Skin with muscle	Skin with muscle
Product functionality	Dressing	Dressing	Dressing	Electromyogram(EMG)	Electromyogram(EMG)

5.3 Performance evaluation of Silbione 4717 adhesive pads

The aging of an adhesive is defined as the change in the quality of the adhesive bonding as a function of storage time and other external factors that promote the change. The purpose of the aging test is to observe and predict the long term performance of adhesives and to propose a solution if necessary [122]. For the Silbione 4717 adhesive pad, its aging was tested after it was exposed to air in laboratory environment for 1 to 7 days [123]. The aging behavior was estimated by measuring peel changes during the 7-day period, as presented in Fig 5.3. The peel strength increased on Day 2 compared to that of Day 1 and then decreased but remained stable between Day 3 to Day 5. On the sixth day, the peel strength suddenly dropped to around 20% of the original strength. The results indicated that the Silbione adhesive was highly sticky for 5 days

with nearly constant peel strength; however, the adhesion strength strongly dropped after 5 days, thus longer term application was not recommended.

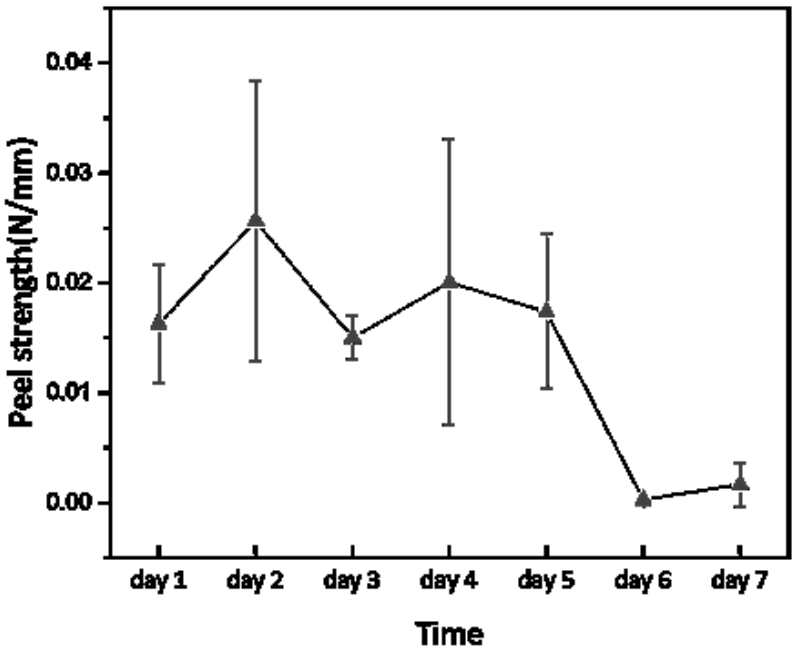

Figure 5.3 The aging test of Silbione 4717 adhesive in ambient environment for 7 days at room temperature, with relative humidity being 20%.

Reusability is an important concern for skin adhesives for most practical applications. In the bonding process, an optimal adhesive is required to flow and deform easily to contact the surface conformably. During the peeling process, on the other hand, it should provide sufficient cohesive strength to prevent a bulk failure, which results in residue formation on skin. In addition, a large energy dissipation is needed so that a greater work of adhesion can be achieved. The peeling process is always accompanied by morphological changes such as fingering, occurrence of a rough surface and particulate contamination, which render the adhesive to lose its adhesion force [124]. In this study, the reusability of Silbione 4717 adhesive was investigated by washing test

and wiping test. In addition, washing test and wiping test were compared to propose a better cleaning method for patients.

In the washing test, the peel test was repeated 4 times after 1 adhesion/debonding cycle, 5 adhesion/debonding cycles, 10 adhesion/debonding cycles, and 20 adhesion/debonding cycles for each washing time/condition to determine the optimal washing time as well as reusability characteristics. Fig 5.4 (a) depicts the washing reusability of the adhesive. Under different washing times/conditions (5, 10, 20, 40-second wash), clear trends in peel strength did not seem to exist. Generally speaking, washing time might have limited impact or no impact on the adhesive's adhesion strength. Within 10 cycles of adhesion/debonding, the adhesive pad showed no systematic change of the peel strength. After 20 cycles, however, the peel strength decreased to ~40% of the original strength. If these adhesive pads were cleaned three times a day with soapy water washing, and the original peel strength was necessary for the application, a week would be the suggested lifetime of the product; however, it must be noted that the values were still considerably bigger than that of Band-Aid®. In summary, we can conclude that the adhesive pad was reusable in a week period or longer and cleaning was possible.

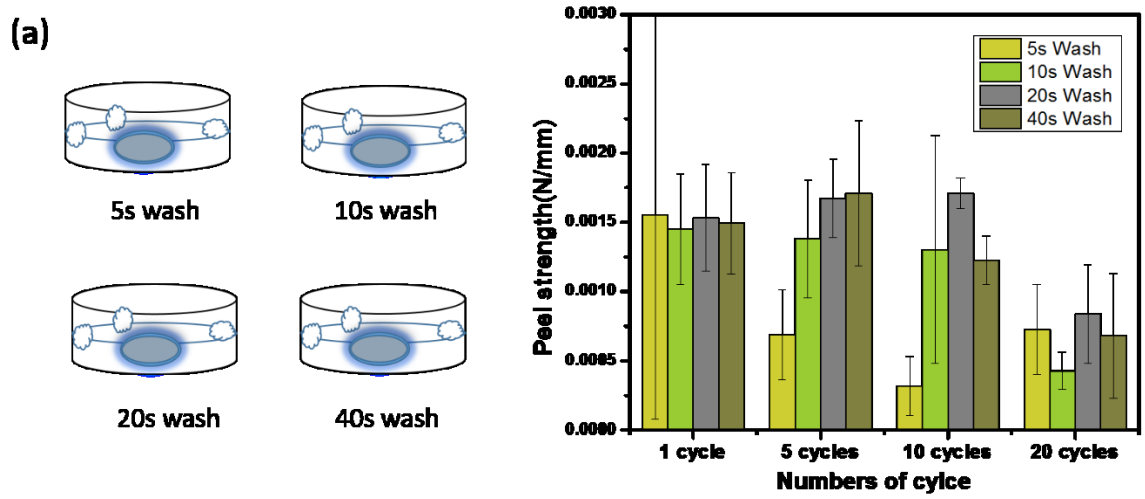

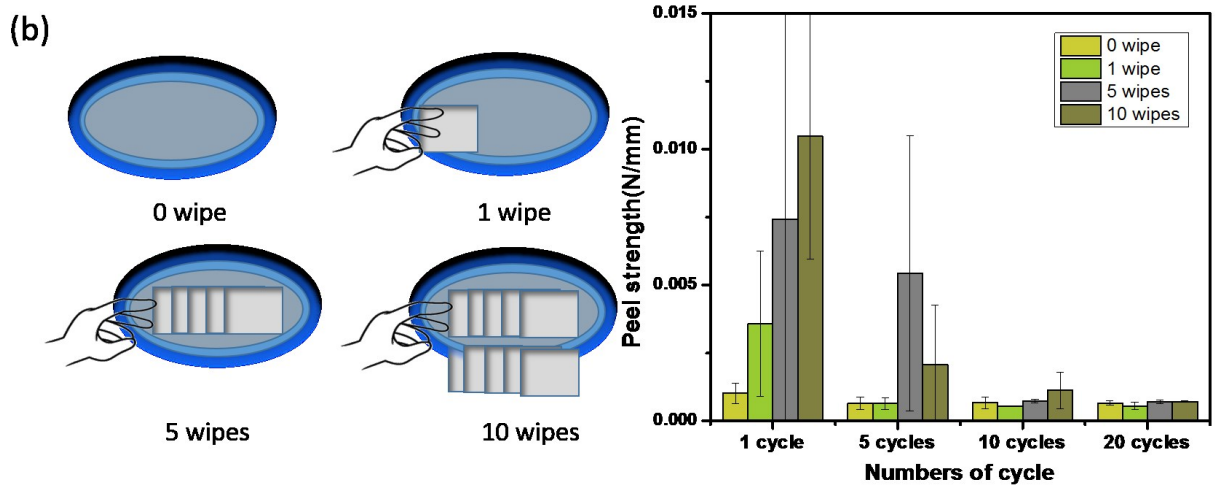

Figure 5.4 Reusability test of Silbione 4717 adhesives. (a) Washing test. (b) Wiping test.

Wiping test in Fig 5.4 (b) is another technique to study the reusability of adhesives. Interestingly, the trend was very different from that of the washing test. In the 1 cycle case, increasing wipe number led to a significant increase of the peel strength. This could possibly indicate that the wiping cleaned the surface contamination so that the effective area of intimate contact increased. After 5 adhesion/debonding cycles, however, 10 wipes sample showed significantly higher rate of decay compared to that of 5 wipe samples. This could possibly be attributed to the damage of the Silbione adhesives layer caused by the isopropyl alcohol swab, leading to reduced peel strength. This was further supported by the fact that all peel strength values were nearly equal after 10 and 20 cycles. After 20 cycles of adhesion/debonding cycles, the peel strength dropped to 10% of its original peel strength. Compared to 1 wipe and 5 wipes, a more prominent loss of peel strength was produced by 10 wipes. Hence 1 wipe and 5 wipes would be recommended for each cleaning, and a three-day lifetime would be suggested.

When comparing soapy water washing with isopropyl alcohol wiping, it was found that the water washing method retained the adhesion strength better during the cleaning process. This might be owing to the mild property of soapy water. Therefore, we would advise using warm soapy water washing for a week to clean the prepared Silbione 4717 adhesive pads.

5.4 Medical grade commercially-available silicone adhesives as alternatives to the Silbione 4717 adhesives

Since the target of our sEMG sensors is to be commercialized and to enter into market, mass production of the adhesives is essential. Therefore, it was necessary to seek medical grade commercially-available silicone adhesives as alternatives to the Silbione 4717 adhesives. A variety of medical adhesives were purchased, and their performances were evaluated by peel test. Results are shown in Fig 5.5. Among these medical adhesives, Scapa RX 1383s® displayed significantly higher peel strength than those of the other materials. As a result, it could be considered as a promising candidate for the adhesive in our sEMG sensor.

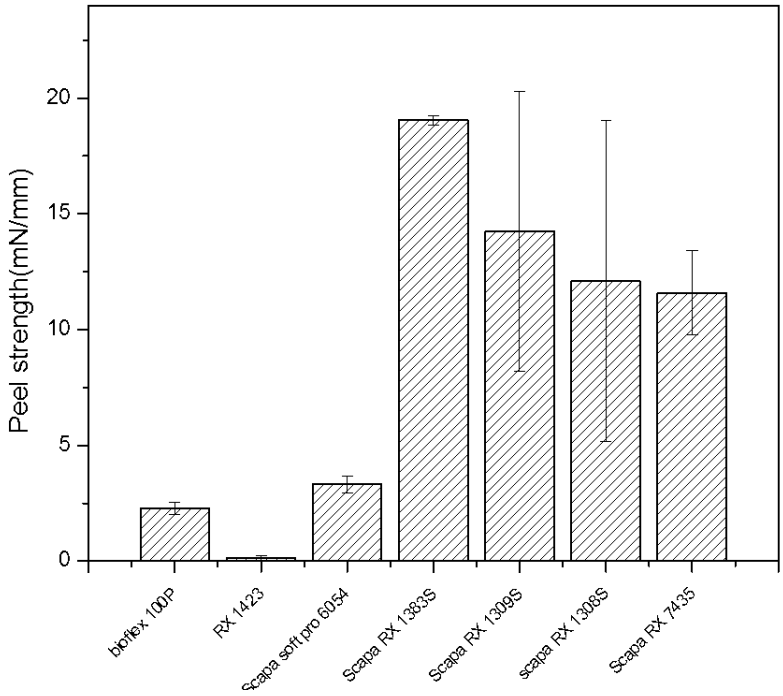

Figure 5.5 The peel strength of various commercial medical grade silicone adhesives.

Finally, a weight loading test was performed by applying Scapa RX 1383 S® adhesives to polypropylene bar. The polypropylene bar was placed on top to simulate skin because its surface energy is around 29 mJ/m^2, which is close to human skin's surface energy of 25 mJ/m^2. The silicone adhesive faced upwards towards the polypropylene surface. Two different weights of stainless steel (28 g and 46 g) were used to represent the weights of two different sEMG sensors. These stainless steel weights were attached at the bottom of the polypropylene bar, while employing the Scapa adhesive at the interface. It was observed that the adhesion was firm for more than a week for both weights. This indicated that adhesion strength provided from the Scapa RX 1383 S® was enough to sustain our sEMG sensor for extended period of time.

5.5 Conclusions

In this work, three types of silicones were evaluated and compared by peel tests. Among them, Silbione 4717 with the thickness range of 640-740 μm was chosen as the raw material to fabricate the adhesive pad for sEMG sensors. The long term performance of adhesives was predicted by an aging test; Reusability of the adhesives was also evaluated by washing and wiping tests; results indicated that the custom-made Silbione 4717 adhesive pad was sticky and reusable. Several medical grade silicone adhesives were compared in order to find an alternative to Silbione adhesive pad. At last, Scapa RX 1383 S® adhesive was considered as the most promising candidate for practical use.

Chapter 6. Summary and future work

The work described in this thesis is focused on multifunctional bionic skin patch. Two themes are included here: the first theme is the preparation and characterization of a pH indicating colorimetric hydrogel, which can be potentially used as wound dressing; the second theme is the evaluation of medical grade silicone adhesive, which will be used for skin electronic application. Nevertheless, some opportunities for extending the scope of this thesis still remain.

6.1 Summary

In theme 1, a series of pH indicating colorimetric alginate/P(AAm-MAPR) hydrogels were synthesized for potential wound dressing application. The pH indicator dye phenol red was successfully modified with methacrylate and subsequently copolymerized into the double network hydrogel matrix. This covalent attachment prevented the dye from leaching out of the matrix. When immersed in buffer solutions with various pH values, the color of the hydrogel dressing underwent a transition from yellow (pH 5, 6 and 7) to bisque (7.4 and 8) and finally to red (pH 9), which matched the required pH range for the application to chronic or infected wounds. The prepared hydrogel dressings showed porous internal structures, excellent mechanical properties, high swelling ratio, and appropriate water vapor transmission rate; these features indicated that the hydrogels were suitable for wound dressing applications. In addition, calcium content could significantly impact the Young's modulus and elongation at break of the hydrogel. In conclusion, our alginate/P(AAm-MAPR) hydrogel could be used as a wound dressing material that allowed monitoring the wound healing process by a simple colorimetric display.

In theme 2, silicone adhesives were prepared as alternatives to acrylic adhesives due to their strong tackiness, nontoxicity and residue-free properties after removal. Three different types of silicones were evaluated and compared. Among them, Silbione 4717 was selected as the raw material to fabricate adhesive pad owing to its high peel strength. The thickness range of 640-740 μm was the best thickness of the adhesive layer, as evidenced by its appropriate peel strength and residue-free property. The long term performance of adhesives was predicted by an aging test; the result indicated that adhesives could remain sticky for 5 days. Reusability of the adhesives was also evaluated by washing and wiping test. Washing was recommended as the cleaning method for the adhesive pad. Since mass production of adhesives is necessary in the future, a commercial replacement to Silbione 4717 must be achieved. Several medical grade silicone adhesives were obtained. Scapa RX 1383 S® was considered as the most promising candidate among these commercial adhesives because it had a significantly higher strength than others. The weight loading test of Scapa RX 1383 S® adhesives was also performed. The adhesion of Scapa RX 1383 S® was firm for more than a week, indicating that its adhesion strength was enough to sustain our sEMG sensor for extended period of time.

6.2 Future work

6.2.1 Sticky hydrogel

The hydrogel used in our research is mechanically strong but lacks bioadhesive strength. A medical tape is always required for anchoring since the adhesive cannot stick to the tissue surface. Therefore, we can design a sticky hydrogel for wound dressing application by tailoring the hydrophilic moieties, such as hydroxyl, ether, amino, and carboxyl groups, existing in the polymeric backbones of hydrogel.

6.2.2 Temperature-sensing hydrogel

Heat is an established marker for indicating the infection in wounds. Before any obvious change occurs to the wound, the changes of temperature may be able to predict the chronicity of wound. Therefore, we can incorporate a temperature sensor to our current pH indicating hydrogel so that a wound dressing with dual responses can be achieved for better wound management.

References

1. Schneider, L.A., et al., *Influence of pH on wound-healing: a new perspective for wound-therapy?* Arch Dermatol Res, 2007. **298**(9): p. 413-20.
2. Gethin, G., *The significance of surface pH in chronic wounds.* Wounds uk, 2007. **3**(3): p. 52.
3. Guinovart, T., et al., *Bandage- Based Wearable Potentiometric Sensor for Monitoring Wound pH.* Electroanalysis, 2014. **26**(6): p. 1345-1353.
4. Schyrr, B., et al., *Development of a polymer optical fiber pH sensor for on-body monitoring application.* Sensors and Actuators B: Chemical, 2014. **194**: p. 238-248.
5. Sridhar, V. and K. Takahata, *A hydrogel-based passive wireless sensor using a flex-circuit inductive transducer.* Sensors and Actuators A: Physical, 2009. **155**(1): p. 58-65.
6. Tamayol, A., et al., *Flexible pH-Sensing Hydrogel Fibers for Epidermal Applications.* Adv Healthc Mater, 2016. **5**(6): p. 711-9.
7. Zheng, A., et al., *Synthesis and characterization of antimicrobial polyvinyl pyrrolidone hydrogel as wound dressing.* Soft Materials, 2014. **12**(3): p. 179-187.
8. Heuss, E., *Die Reaktion des Schweisses beim gesunden Menschen*. 1892: Voss.
9. Schade, H. and A. Marchionini, *Der Säuremantel der Haut (nach Gaskettenmessungen).* Journal of Molecular Medicine, 1928. **7**(1): p. 12-14.
10. Dikstein, S. and A. Zlotogorski, *Measurement of skin pH.* Acta dermato-venereologica. Supplementum, 1993. **185**: p. 18-20.
11. Lambers, H., et al., *Natural skin surface pH is on average below 5, which is beneficial for its resident flora.* International journal of cosmetic science, 2006. **28**(5): p. 359-370.
12. Parra, J. and M. Paye, *EEMCO guidance for the in vivo assessment of skin surface pH.* Skin Pharmacology and Physiology, 2003. **16**(3): p. 188-202.
13. Yosipovitch, G. and H. Maibach, *Skin surface pH: A protective acid mantle: An acidic skin-surface pH promotes barrier function and fights infection.* Cosmetics and toiletries, 1996. **111**(12): p. 101-102.
14. Visscher, M.O., et al., *Changes in diapered and nondiapered infant skin over the first month of life.* Pediatric dermatology, 2000. **17**(1): p. 45-51.

15. Zlotogorski, A., *Distribution of skin surface pH on the forehead and cheek of adults.* Archives of dermatological research, 1987. **279**(6): p. 398-401.
16. Dikstein, S. and A. Zlotogorski, *Skin surface hydrogen ion concentration (pH).* Cutaneous Investigation in Health and Disease, 1989: p. 59-77.
17. Wesley, N.O. and H.I. Maibach, *Racial (ethnic) differences in skin properties.* American journal of clinical dermatology, 2003. **4**(12): p. 843-860.
18. Schmid-Wendtner, M.H. and H.C. Korting, *The pH of the skin surface and its impact on the barrier function.* Skin Pharmacol Physiol, 2006. **19**(6): p. 296-302.
19. Barel, A., et al., *A comparative study of the effects on the skin of a classical bar soap and a syndet cleansing bar in normal use conditions and in the soap chamber test.* Skin Research and Technology, 2001. **7**(2): p. 98-104.
20. Korting, H.C. and O. Braun-Falco, *The effect of detergents on skin pH and its consequences.* Clinics in dermatology, 1996. **14**(1): p. 23-27.
21. Stenzaly- Achtert, S., et al., *Axillary pH and influence of deodorants.* Skin Research and Technology, 2000. **6**(2): p. 87-91.
22. Hartmann, A., *Effect of occlusion on resident flora, skin-moisture and skin-pH.* Archives of dermatological research, 1983. **275**(4): p. 251-254.
23. Redoules, D., R. Tarroux, and J. Perie, *Epidermal enzymes: their role in homeostasis and their relationships with dermatoses.* Skin Pharmacology and Physiology, 1999. **11**(4-5): p. 183-192.
24. Mauro, T., et al., *Barrier recovery is impeded at neutral pH, independent of ionic effects: implications for extracellular lipid processing.* Archives of dermatological research, 1998. **290**(4): p. 215-222.
25. Leyvraz, C., et al., *The epidermal barrier function is dependent on the serine protease CAP1/Prss8.* The Journal of cell biology, 2005. **170**(3): p. 487-496.
26. Schreml, S., et al., *The impact of the pH value on skin integrity and cutaneous wound healing.* J Eur Acad Dermatol Venereol, 2010. **24**(4): p. 373-8.
27. O'Meara, S., et al., *Systematic reviews of wound care management:(3) antimicrobial agents for chronic wounds;(4) diabetic foot ulceration.* Health technology assessment (Winchester, England), 1999. **4**(21): p. 1-237.

28. Thomas, L.V., J.W. Wimpenny, and J.G. Davis, *Effect of three preservatives on the growth of Bacillus cereus, Vero cytotoxigenic Escherichia coli and Staphylococcus aureus, on plates with gradients of pH and sodium chloride concentration.* International journal of food microbiology, 1993. **17**(4): p. 289-301.
29. Stüttgen, G., *Haut und Alter*, in *Funktionelle Dermatologie*. 1974, Springer. p. 312-317.
30. Greener, B., A. Hughes, and N. Bannister. *The effect of pH on proteolytic activity in chronic wound fluids and methods for determination*. in *Poster Z079 2nd WUWHS Congress, Paris*. 2005.
31. Wilson, I., et al., *The pH of varicose ulcer surfaces and its relationship to healing.* VASA. Zeitschrift fur Gefasskrankheiten, 1978. **8**(4): p. 339-342.
32. Glibbery, A. and R. Mani, *pH in leg ulcers.* Int J Microcirc Clin Exp, 1992. **2**(109): p. 98.
33. Greener, B., et al., *Proteases and pH in chronic wounds.* Journal of wound care, 2005. **14**(2): p. 59-61.
34. Leveen, H.H., et al., *Chemical acidification of wounds. An adjuvant to healing and the unfavorable action of alkalinity and ammonia.* Annals of surgery, 1973. **178**(6): p. 745.
35. Trengove, N., et al., *Qualitative bacteriology and leg ulcer healing.* Journal of wound care, 1996. **5**(6): p. 277-280.
36. Hunt, T. and S. Beckert, *Therapeutical and practical aspects of oxygen in wound healing.* The Wound Management Manual. McGraw-Hill Medical, New York, 2005.
37. Thomas, S., *Wound management and dressings*. 1990: Pharmaceutical Press.
38. Gethin, G. and S. Cowman. *Changes in surface pH of chronic wounds when a honey dressing was used*. in *Wounds UK Conference Proceedings*. 2006.
39. Romanelli, M. *Evaluation of surface pH on venous leg ulcers under Allevyn dressings*. in *International congress and symposium series-royal society of medicine*. 1998. Royal society of medicine services ltd.
40. Varghese, M.C., et al., *Local environment of chronic wounds under synthetic dressings.* Archives of dermatology, 1986. **122**(1): p. 52-57.
41. Sharp, D., *Printed composite electrodes for in-situ wound pH monitoring.* Biosensors and Bioelectronics, 2013. **50**: p. 399-405.
42. Arshak, K., et al., *Investigation of tin oxides as sensing layers in conductimetric interdigitated pH sensors.* Sensors and Actuators B: Chemical, 2007. **127**(1): p. 42-53.

43. Robinson, K.L. and N.S. Lawrence, *Redox-sensitive copolymer: A single-component pH sensor.* Analytical chemistry, 2006. **78**(7): p. 2450-2455.
44. Korostynska, O., et al., *Review on state-of-the-art in polymer based pH sensors.* Sensors, 2007. **7**(12): p. 3027-3042.
45. Trupp, S., et al., *Development of pH-sensitive indicator dyes for the preparation of micro-patterned optical sensor layers.* Sensors and Actuators B: Chemical, 2010. **150**(1): p. 206-210.
46. Dargaville, T.R., et al., *Sensors and imaging for wound healing: a review.* Biosensors and Bioelectronics, 2013. **41**: p. 30-42.
47. Van der Schueren, L. and K. De Clerck, *Coloration and application of pH-sensitive dyes on textile materials.* Coloration Technology, 2012. **128**(2): p. 82-90.
48. Cho, C.Y. and J.S. Lo, *Dressing the part.* Dermatologic clinics, 1998. **16**(1): p. 25-47.
49. Ovington, L., *The well-dressed wound: an overview of dressing types.* Wounds, 1998. **10**(suppl A): p. 1A-11A.
50. Turner, T., *The development of wound management products.* Wounds, 1989. **1**(3): p. 155-171.
51. Winter, G.D., *Formation of the scab and the rate of epithelization of superficial wounds in the skin of the young domestic pig.* 1962.
52. Winter, G.D., *Effect of air exposure and occlusion on experimental human skin wounds.* Nature, 1963. **200**: p. 378-379.
53. Bolton, L., K. Monte, and L. Pirone, *Moisture and healing: beyond the jargon.* Ostomy/wound management, 2000. **46**(1A Suppl): p. 51S-62S; quiz 63S-64S.
54. Field, C.K. and M.D. Kerstein, *Overview of wound healing in a moist environment.* The American journal of surgery, 1994. **167**(1): p. S2-S6.
55. Kannon, G.A. and A.B. Garrett, *Moist wound healing with occlusive dressings.* Dermatologic surgery, 1995. **21**(7): p. 583-590.
56. Hutchinson, J. and M. McGuckin, *Occlusive dressings: a microbiologic and clinical review.* American journal of infection control, 1990. **18**(4): p. 257-268.
57. Werner, S. and R. Grose, *Regulation of wound healing by growth factors and cytokines.* Physiological reviews, 2003. **83**(3): p. 835-870.

58. Seaman, S., *Dressing selection in chronic wound management.* Journal of the American Podiatric Medical Association, 2002. **92**(1): p. 24-33.

59. Rolstad, B.S., et al., *Principles of wound management*. 2007: Mosby Elsevier Missouri MA.

60. Krasner, D., *AHCPR Clinical Practice Guideline Number 15, Treatment of Pressure Ulcers: a pragmatist's critique for wound care providers.* Ostomy/wound management, 1995. **41**(7A Suppl): p. 97S-101S; discussion 102S.

61. Skorkowska-Telichowska, K., et al., *The local treatment and available dressings designed for chronic wounds.* J Am Acad Dermatol, 2013. **68**(4): p. e117-26.

62. Barnea, Y., J. Weiss, and E. Gur, *A review of the applications of the hydrofiber dressing with silver (Aquacel Ag®) in wound care.* Therapeutics and clinical risk management, 2010. **6**: p. 21.

63. Robinson, B., *The use of a hydrofibre dressing in wound management.* Journal of wound care, 2000. **9**(1): p. 32-34.

64. Palamand, S., R. Brenden, and A. Reed, *Intelligent wound dressings and their physical characteristics.* Wounds: a compendium of clinical research and practice, 1992. **3**(4): p. 149-156.

65. Ponder, R. and D. Krasner, *Gauzes and related dressings.* Ostomy/wound management, 1993. **39**(5): p. 48.

66. Weir, D., et al., *Improved wound packing and debriment-evaluation of a new fabric sponge.* Wounds-a compendium of clinical research and practice, 1992. **4**(6): p. 216-226.

67. Lawrence, J.C., *Dressings and wound infection.* The American journal of surgery, 1994. **167**(1): p. S21-S24.

68. Khademhosseini, A. and R. Langer, *Microengineered hydrogels for tissue engineering.* Biomaterials, 2007. **28**(34): p. 5087-5092.

69. Khademhosseini, A., et al., *Microscale technologies for tissue engineering and biology.* Proceedings of the National Academy of Sciences of the United States of America, 2006. **103**(8): p. 2480-2487.

70. Seliktar, D., *Designing cell-compatible hydrogels for biomedical applications.* Science, 2012. **336**(6085): p. 1124-1128.

71. Sun, J.Y., et al., *Highly stretchable and tough hydrogels.* Nature, 2012. **489**(7414): p. 133-6.

72. Yang, C.H., et al., *Strengthening alginate/polyacrylamide hydrogels using various multivalent cations.* ACS applied materials & interfaces, 2013. **5**(21): p. 10418-10422.

73. Yang, C.H., et al., *Strengthening alginate/polyacrylamide hydrogels using various multivalent cations.* ACS Appl Mater Interfaces, 2013. **5**(21): p. 10418-22.

74. Kermis, H.R., Y. Kostov, and G. Rao, *Rapid method for the preparation of a robust optical pH sensor.* The Analyst, 2003. **128**(9): p. 1181.

75. Fan, Z., et al., *A Novel Wound Dressing Based on Ag/Graphene Polymer Hydrogel: Effectively Kill Bacteria and Accelerate Wound Healing.* Advanced Functional Materials, 2014. **24**(25): p. 3933-3943.

76. Bajpai, S.K., et al., *CNWs loaded poly(SA) hydrogels: effect of high concentration of CNWs on water uptake and mechanical properties.* Carbohydr Polym, 2014. **106**: p. 351-8.

77. Gong, J.P., et al., *Double- network hydrogels with extremely high mechanical strength.* Advanced Materials, 2003. **15**(14): p. 1155-1158.

78. Shezad, O., et al., *Physicochemical and mechanical characterization of bacterial cellulose produced with an excellent productivity in static conditions using a simple fed-batch cultivation strategy.* Carbohydrate Polymers, 2010. **82**(1): p. 173-180.

79. Zhang, D., et al., *Carboxyl-modified poly (vinyl alcohol)-crosslinked chitosan hydrogel films for potential wound dressing.* Carbohydrate polymers, 2015. **125**: p. 189-199.

80. Roy, N., et al., *Permeability and biocompatibility of novel medicated hydrogel wound dressings.* Soft Materials, 2010. **8**(4): p. 338-357.

81. Lamke, L.-O., G. Nilsson, and H. Reithner, *The evaporative water loss from burns and the water-vapour permeability of grafts and artificial membranes used in the treatment of burns.* Burns, 1977. **3**(3): p. 159-165.

82. Tsao, C.T., et al., *Evaluation of chitosan/γ-poly (glutamic acid) polyelectrolyte complex for wound dressing materials.* Carbohydrate polymers, 2011. **84**(2): p. 812-819.

83. Bajpai, S., et al., *CNWs loaded poly (SA) hydrogels: effect of high concentration of CNWs on water uptake and mechanical properties.* Carbohydrate polymers, 2014. **106**: p. 351-358.

84. Boateng, J.S., et al., *Wound healing dressings and drug delivery systems: a review.* Journal of pharmaceutical sciences, 2008. **97**(8): p. 2892-2923.

85. Lansdown, A.B., *Calcium: a potential central regulator in wound healing in the skin.* Wound repair and regeneration, 2002. **10**(5): p. 271-285.

86. Kamoun, E.A., et al., *Crosslinked poly (vinyl alcohol) hydrogels for wound dressing applications: A review of remarkably blended polymers.* Arabian Journal of Chemistry, 2015. **8**(1): p. 1-14.

87. Venkatraman, S. and R. Gale, *Skin adhesives and skin adhesion: 1. Transdermal drug delivery systems.* Biomaterials, 1998. **19**(13): p. 1119-1136.

88. Rippon, M., R. White, and P. Davies, *Skin adhesives and their role in wound dressings.* WOUNDS UK, 2007. **3**(4): p. 76.

89. Bagley, D., et al., *Skin irritation: reference chemicals data bank.* Toxicology in Vitro, 1996. **10**(1): p. 1-6.

90. Prevo, M., M. Cormier, and K. Nichols, *Predictive Toxicology Methods for Transdermal Delivery Systems.* Toxicology Methods, 1996. **6**(2): p. 83-98.

91. Convention, U.S.P., *About USP.*

92. Moore, D.R., J. Williams, and A. Pavan, *Fracture mechanics testing methods for polymers, adhesives and composites*. Vol. 28. 2001: Elsevier.

93. Kinloch, A., *The science of adhesion.* Journal of materials science, 1980. **15**(9): p. 2141-2166.

94. Borroff, E. and W. Wake, *Adhesion of Rubber and Textiles. II. Factors Influencing the Load Required to Strip Rubber from Fabric and Foil Surfaces.* Rubber Chemistry and Technology, 1950. **23**(2): p. 482-490.

95. Patrick, R.L., *Treatise on adhesion and adhesives*. Vol. 5. 1981: CRC Press.

96. Wake, W.C., *Adhesion and the Formulation of Adhesives*. 1976, London: Applied science. 69.

97. Voiutskii, S.S., *Autohesion and adhesion of high polymers.* 1963.

98. Lee, L.-H., *Theory of the effect of phase transition on liquid surface tension.* Journal of Colloid and Interface Science, 1971. **37**(4): p. 653-658.

99. Anand, J. and H. Kabam, *Interfacial Contact and Bonding in Autohesion I-Contact Theory.* The Journal of Adhesion, 1969. **1**(1): p. 16-23.

100. Campion, R., *The influence of structure on autohesion (self-tack) and other forms of diffusion into polymers.* The Journal of Adhesion, 1975. **7**(1): p. 1-23.

101. Vasenin, R., *Adhesion, Fundamentals and Practice*. Ministry of Technology, MacLaren, London. 1969, London: McLaren and Son.

102. Von Harrach, H.G. and B. Chapman, *Charge effects in thin film adhesion.* Thin Solid Films, 1972. **13**(1): p. 157-161.

103. Schnabel, W., *Physics of Adhesion.* Universit/it Karlsruhe, Karlsruhe, 1969) p, 1969. **102**.

104. ELEY, D.D., *Adhesion. Edited by DD Eley... for the Adhesion Panel of the Advisory Council on Scientific Research and Technical Development.[By Various Authors.]*. 1961, London: Oxford University Press.

105. Staverman, A., N. DeBruyne, and R. Houwink, *Adhesion and Adhesives*. 1965, Vol. I, edited by R. Houwink and G. Salmon, Elsevier, Amsterdam.

106. Huntsberger, J. and R. Patrick, *Treatise on adhesion and adhesives.* Ed. PATRICK, RL DEKKER, M., New York, 1967. **1**: p. 119.

107. Bolger, J., A. Michaels, and P. Weiss, *Interface conversion for polymer coatings.* Weiss and Cheever, eds., Elsivier, New York, 1968.

108. Koenig, J. and P.T. Shih, *Raman studies of the glass fiber-silane-resin interface.* Journal of Colloid and Interface Science, 1971. **36**(2): p. 247-253.

109. Bailey, R. and J. Castle, *XPS study of the adsorption of ethoxysilanes on iron.* Journal of Materials Science, 1977. **12**(10): p. 2049-2055.

110. Werner, H., *Quantitative secondary ion mass spectrometry: A review.* Surface and Interface Analysis, 1980. **2**(2): p. 56-74.

111. Safetac, M.B. and D.E. Thin, *E ffects of adhesive dressings on the stratum corneum of the skin.* 2001.

112. Dykes, P., *Theeffect of adhesive dressing edges on cutaneous irritancy and skin barrierfunction.* 2007.

113. Maume, S., et al., *A study to compare a new self-adherent soft silicone dressing with a self-adherent polymer dressing in stage II pressure ulcers.* Ostomy/wound management, 2003. **49**(9): p. 44-51.

114. Thomas, S., *Soft silicone dressings: frequently asked questions.* World Wide Wounds. Available online at: www. worldwidewounds. com/2003/october/thomas/soft-silicone-faq. hmtl, 2003.

115. Dykes, P. and R. Heggie, *The link between the peel force of adhesive dressings and subjective discomfort in volunteer subjects.* Journal of Wound Care, 2003. **12**(7): p. 260-262.

116. Zillmer, R., et al., *Biophysical effects of repetitive removal of adhesive dressings on peri-ulcer skin.* Journal of Wound Care, 2006. **15**(5): p. 187-191.

117. Milne, C.T. and L.Q. Corbett, *A new option in the treatment of skin tears for the institutionalized resident: formulated 2-octylcyanoacrylate topical bandage.* Geriatric Nursing, 2005. **26**(5): p. 321-325.

118. Silvestri, A., et al., *Octyl-2-cyanoacrylate adhesive for skin closure and prevention of infection in plastic surgery.* Aesthetic plastic surgery, 2006. **30**(6): p. 695-699.

119. Anseth, K.S., C.N. Bowman, and L. Brannon-Peppas, *Mechanical properties of hydrogels and their experimental determination.* Biomaterials, 1996. **17**(17): p. 1647-1657.

120. Oyen, M., *Mechanical characterisation of hydrogel materials.* International Materials Reviews, 2014. **59**(1): p. 44-59.

121. Silicones, B. *Skin adhesives*. Available from: http://www.silbione.com/products/skin-adhesives.

122. *Ageing test - Adhesive bonding aging test*. Available from: http://www.adhesiveandglue.com/ageing-testing.html.

123. Benedek, I., *Pressure-sensitive adhesives and applications*. 2004: CRC Press.

124. Patil, S., et al., *Reusable antifouling viscoelastic adhesive with an elastic skin.* Langmuir, 2011. **28**(1): p. 42-46.

Appendix

Peel strength analysis

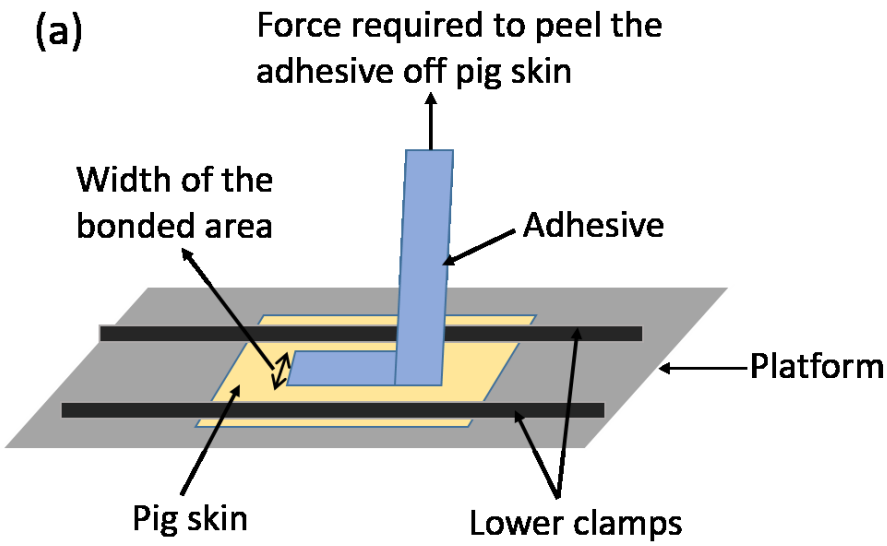

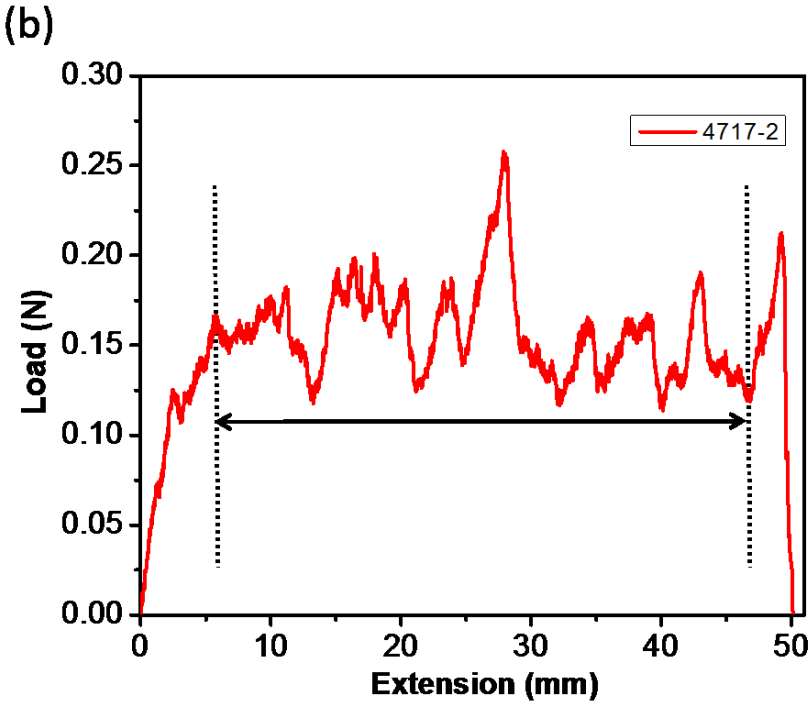

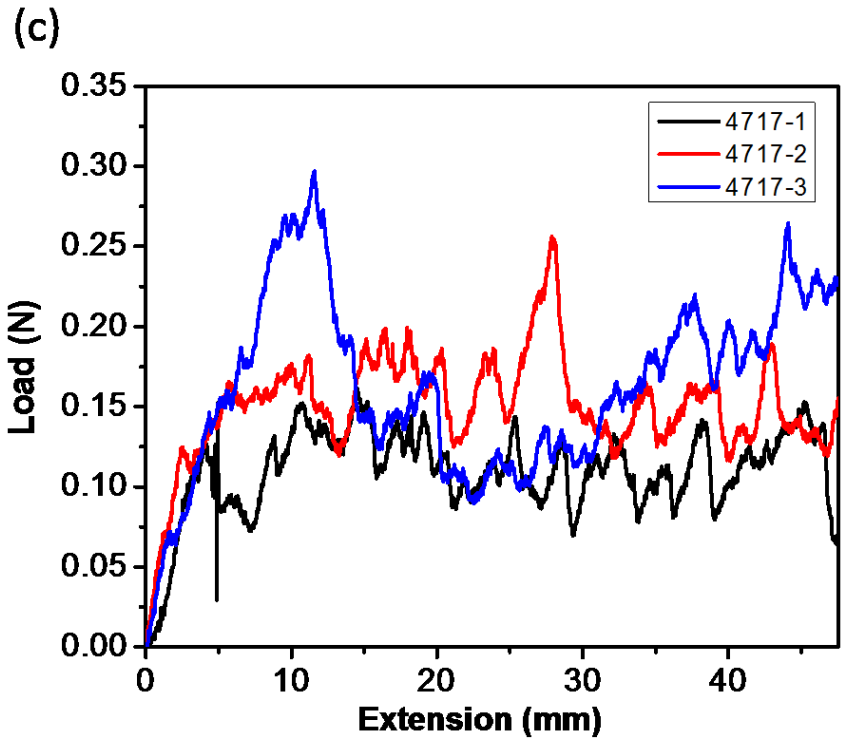

Figure A-1. (a) The set-up of a 90° peel test. (b) The representative graph of a peel test of a Silbione 4717 adhesive pad. (c) Three overlapping peel tests of Silbione 4717 adhesive pads.

A 90° peel test was performed using the Instron 5943 with a 1 kN load cell (Fig A-1(a)). The pig skin was secured to a platform, and the adhesive pad was then placed on the pig skin. The other end of the adhesive pad was secured in a set of upper clamps of the peel tester. The adhesive pad was peeled mechanically off the pig skin at a speed of 10 mm min^{-1}.

One example of the peel strength analysis was the Silbione 4717 adhesive pad with a thickness range of 240-340 µm, as shown in Fig A-1 (b) and (c). The average peel strength of this adhesive pad was calculated by measuring the average load of the peel test (Fig A-1 (b)) and dividing it by the width of the bond area (Fig A-1 (a)). Ideally, the peel strength was supposed to be consistent

throughout the three repeated measurements to ensure the reproducibility (Fig A-1 (c)). In the last, an average peel strength could be determined from the three repeated measurements.